

The contact ratio  $m_P$  in the transverse plane (profile-contact ratio) is defined as the ratio of the total length of the line of action in the transverse plane  $Z$  to the base pitch in the transverse plane  $p_b$ . Thus

$$m_P = \frac{Z}{p_b} \quad (10.8)$$

The diametral pitch, pitch diameters, helix angle, and normal pressure angle at the operating pitch circle are required in the load-capacity evaluation of helical gears. These terms are given by

$$P_{do} = \frac{N_P + N_G}{2C_o} \quad (10.9)$$

for external mesh; for internal mesh,

$$P_{do} = \frac{N_G - N_P}{2C_o} \quad (10.10)$$

Also,

$$d = \frac{N_P}{P_{do}} \quad D = \frac{N_G}{P_{do}} \quad (10.11)$$

$$\psi_B = \tan^{-1} (\tan \psi \cos \phi_T) \quad (10.12)$$

$$\psi_o = \tan^{-1} \frac{\tan \psi_B}{\cos \phi_o} \quad (10.13)$$

$$\phi_{No} = \sin^{-1} (\sin \phi_o \cos \psi_B) \quad (10.14)$$

where  $P_{do}$  = operating diametral pitch  
 $\psi_B$  = base helix angle, deg  
 $\psi_o$  = helix angle at operating pitch point, deg  
 $\phi_{No}$  = operating normal pressure angle, deg  
 $d$  = operating pinion pitch diameter, in  
 $D$  = operating gear pitch diameter, in

## 10.5 LOAD RATING

---

Reference [10.1] establishes a coherent method for rating external helical and spur gears. The treatment of strength and durability provided here is derived in large part from this source.

Four factors must be considered in the load rating of a helical-gear set: strength, durability, wear resistance, and scoring probability. Although strength and durability must always be considered, wear resistance and scoring evaluations may not be required for every case. We treat each topic in some depth.

### 10.5.1 Strength and Durability

The strength of a gear tooth is evaluated by calculating the bending stress index number at the root by

$$s_t = \frac{W_t K_a}{K_v} \frac{P_d}{F_E} \frac{K_b K_m}{J} \quad (10.15)$$

where  $s_t$  = bending stress index number, pounds per square inch (psi)

$K_a$  = bending application factor

$F_E$  = effective face width, in

$K_m$  = bending load-distribution factor

$K_v$  = bending dynamic factor

$J$  = bending geometry factor

$P_d$  = transverse operating diametral pitch

$K_b$  = rim thickness factor

The calculated bending stress index number  $s_t$  must be within safe operating limits as defined by

$$s_t \leq \frac{s_{at} K_L}{K_T K_R} \quad (10.16)$$

where  $s_{at}$  = allowable bending stress index number

$K_L$  = life factor

$K_T$  = temperature factor

$K_R$  = reliability factor

Some of the factors which are used in these equations are similar to those used in the durability equations. Thus we present the basic durability rating equations before discussing the factors:

$$s_c = C_p \sqrt{\frac{W_t C_a}{C_v} \frac{1}{d F_N} \frac{C_m}{I}} \quad (10.17)$$

where  $s_c$  = contact stress index number

$C_a$  = durability application factor

$C_v$  = durability dynamic factor

$d$  = operating pinion pitch diameter

$F_N$  = net face width, in

$C_m$  = load-distribution factor

$C_p$  = elastic coefficient

$I$  = durability geometry factor

The calculated contact stress index number must be within safe operating limits as defined by

$$s_c \leq \frac{s_{ac} C_L C_H}{C_T C_R} \quad (10.18)$$

where  $s_{ac}$  = allowable contact stress index number

$C_L$  = durability life factor

$C_H$  = hardness ratio factor

$C_T$  = temperature factor

$C_R$  = reliability factor

To utilize these equations, each factor must be evaluated. The tangential load  $W_t$  is given by

$$W_t = \frac{2T_P}{d} \quad (10.19)$$

where  $T_P$  = pinion torque in inch-pounds (in · lb) and  $d$  = pinion operating pitch diameter in inches. If the duty cycle is not uniform but does not vary substantially, then the maximum anticipated load should be used. Similarly, if the gear set is to operate at a combination of very high and very low loads, it should be evaluated at the maximum load. If, however, the loading varies over a well-defined range, then the cumulative fatigue damage for the loading cycle should be evaluated by using Miner's rule. For a good explanation, see Ref. [10.2].

**Application Factors  $C_a$  and  $K_a$ .** The application factor makes the allowances for externally applied loads of unknown nature which are in excess of the nominal tangential load. Such factors can be defined only after considerable field experience has been established. In a *new* design, this consideration places the designer squarely on the horns of a dilemma, since "new" presupposes limited, if any, experience. The values shown in Table 10.3 may be used as a guide if no other basis is available.

**TABLE 10.3** Application Factor Guidelines

Power source	Character of load on driven machine		
	Uniform	Moderate shock	Heavy shock
Uniform	1.15	1.25	At least 1.75
Light shock	1.25	1.50	At least 2.00
Medium shock	1.50	1.75	At least 2.50

The application factor should never be set equal to unity except where clear experimental evidence indicates that the loading will be absolutely uniform. Whenever possible, the actual loading to be applied to the system should be defined. One of the most common mistakes made by gear system designers is assuming that the motor (or engine, etc.) "nameplate" rating is also the gear unit rating point.

**Dynamic Factors  $C_v$  and  $K_v$ .** These factors account for internally generated tooth loads which are induced by nonconjugate meshing action. This discontinuous motion occurs as a result of various tooth errors (such as spacing, profile, and runout) and system effects (such as deflections). Other effects, such as system torsional resonances and gear blank resonant responses, may also contribute to the overall dynamic loading experienced by the teeth. The latter effects must, however, be separately evaluated. The effect of tooth accuracy may be determined from Fig. 10.4, which is based on both pitch line velocity and gear quality  $Q_n$  as specified in Ref. [10.3]. The pitch line velocity of a gear is

$$v_t = 0.2618nD \quad (10.20)$$

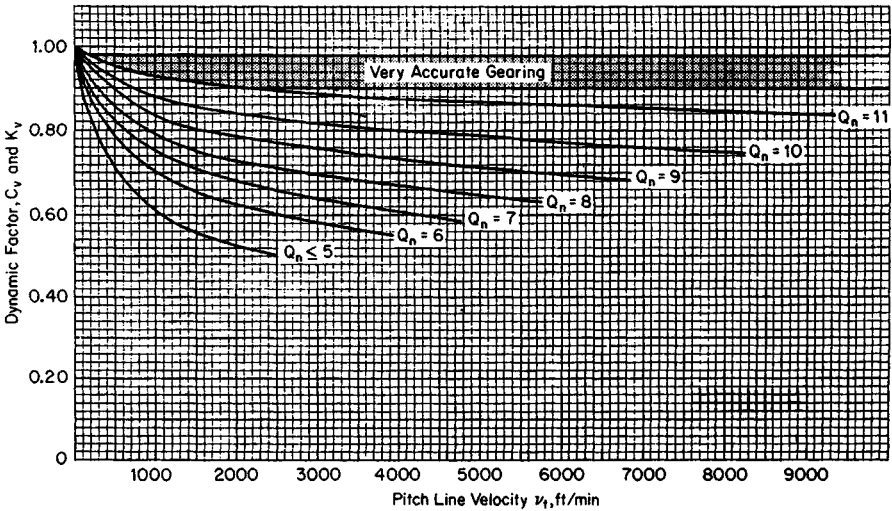


FIGURE 10.4 Dynamic factors  $C_v$  and  $K_v$ . (From Ref. [10.1].)

where  $v_1$  = pitch line velocity, feet per minute (ft/min)  
 $n$  = gear speed, revolutions per minute (r/min)  
 $D$  = gear pitch diameter, in

**Effective and Net Face Widths  $F_E$  and  $F_N$ .** The net minimum face width of the narrowest member should always be used for  $F_N$ . In cases where one member has a substantially larger face width than its mate, some advantage may be taken of this fact in the bending stress calculations, but it is unlikely that a very narrow tooth will fully transfer its tooth load across the face width of a much wider gear. At best, the effective face width of a larger-face-width gear mating with a smaller-face-width gear is limited to the minimum face of the smaller member plus some allowance for the extra support provided by the wide face. Figure 10.5 illustrates the definition of net and effective face widths for various cases.

**Rim Thickness Factor  $K_b$ .** The basic bending stress equations were developed for a single tooth mounted on a rigid support so that it behaves as a short cantilever beam. As the rim which supports the gear tooth becomes thinner, a point is reached at which the rim no longer provides “rigid” support. When this occurs, the bending of the rim itself combines with the tooth bending to yield higher total alternating stresses than would be predicted by the normal equations. Additionally, when a tooth is subjected to fully reversed bending loads, the alternating stress is also increased because of the additive effect of the compressive stress distribution on the normally unloaded side of the tooth, as Fig. 10.6 shows. Both effects are accounted for by the rim thickness factor, as Fig. 10.7 indicates.

It must be emphasized that the data shown in Fig. 10.7 are based on a limited amount of analytical and experimental (photoelastic and strain-gauge) measurements and thus must be used judiciously. Still, they are the best data available to date and are far better than nothing at all; see Refs. [10.4] and [10.5].

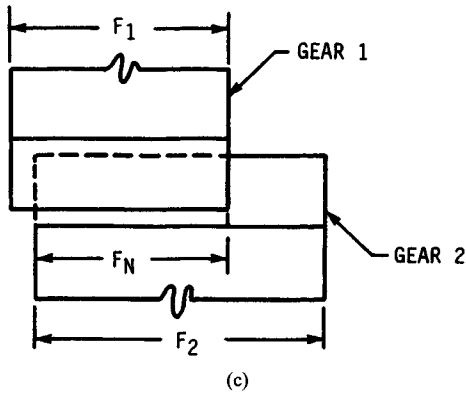
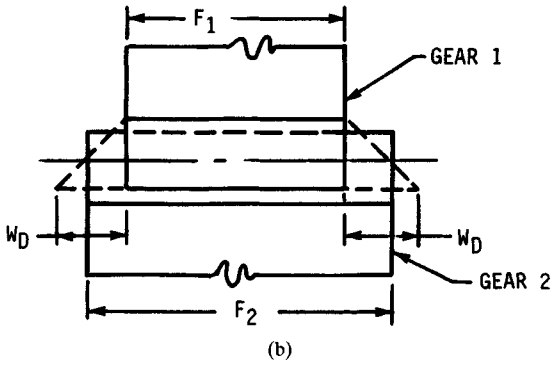
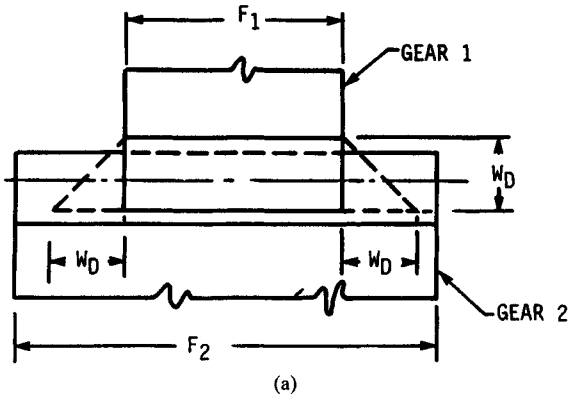


**FIGURE 10.5** Definition of effective face width. (a)  $F_{E1} = F_1, F_{E2} = F_1 + 2W_D; F_N = F_1$ ; (b)  $F_{E1} = F_1, F_{E2} = F_2, F_N = F_1$ ; (c)  $F_{E1} = F_{E2} = F_N$ .

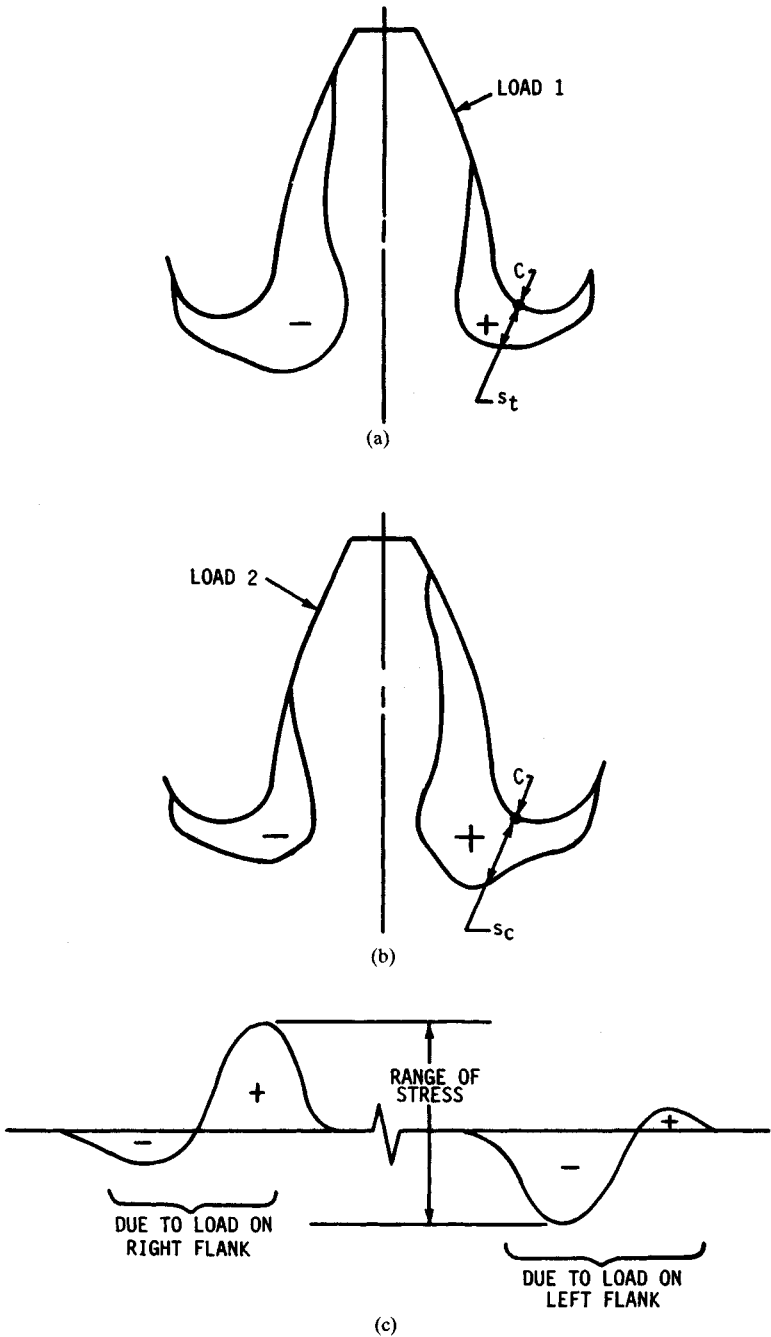


**FIGURE 10.6** Stress condition for reversing (as with an idler) loading. (a) Load on right flank; (b) load on left flank; (c) typical waveform for strain gauge at point C.

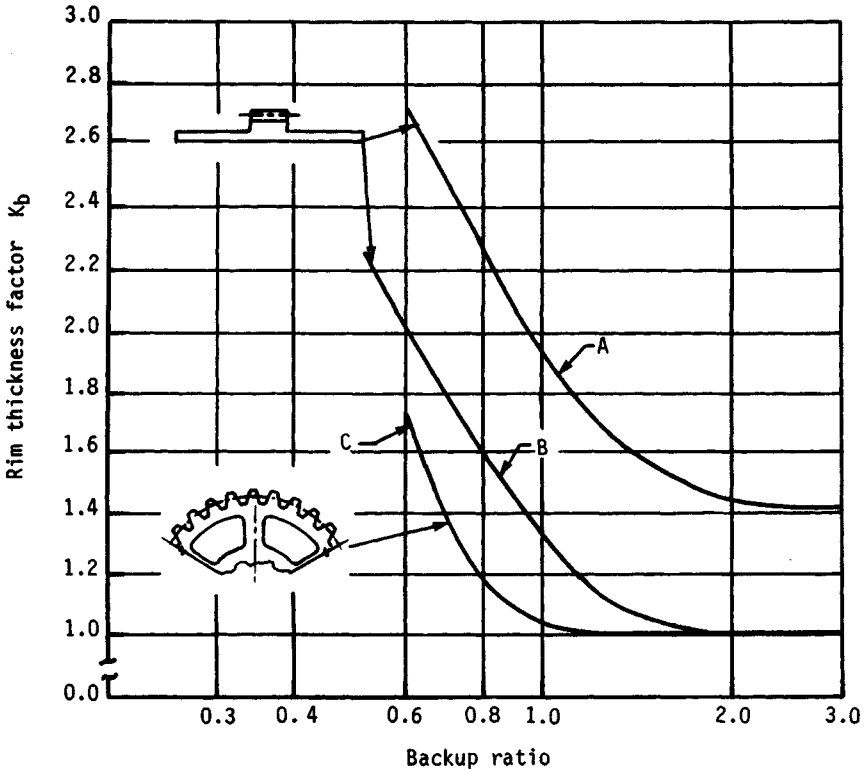


**FIGURE 10.7** Rim thickness factor  $K_b$ . The *backup ratio* is defined as the ratio of the rim thickness to the tooth height. Curve A is fully reversed loading; curves B and C are unidirectional loading.

For gear blanks which utilize a T-shaped rim and web construction, the web acts as a hard point, if the rim is thin, and stresses will be higher over the web than over the ends of the T. The actual value which should be used for such constructions depends greatly on the relative proportions of the gear face width and the web. If the web spans 70 to 80 percent of the face width, the gear may be considered as having a rigid backup. Thus the backup ratio will be greater than 2.0, and any of the curves shown may be used (that is, curve C or B, both of which are identical above a 2.0 backup ratio, for unidirectional loading or curve A for fully reversed loading). If the proportions are between these limits, the gear lies in a gray area and probably lies somewhere in the range defined by curves B and C. Some designer discretion should be exercised here.

Finally, note that the rim thickness factor is equal to unity only for unidirectionally loaded, rigid-backup helical gears. For fully reversed loading, its value will be at least 1.4, even if the backup is rigid.

**Load-Distribution Factors  $K_m$  and  $C_e$ .** These factors modify the rating equations to account for the manner in which the load is distributed on the teeth. The load on a set of gears will never be exactly uniformly distributed. Factors which affect the load distribution include the accuracy of the teeth themselves; the accuracy of the

housing which supports the teeth (as it influences the alignment of the gear axes); the deflections of the housing, shafts, and gear blanks (both elastic and thermal); and the internal clearances in the bearings which support the gears, among others.

All these and any other appropriate effects must be evaluated in order to define the total effective alignment error  $e_t$  for the gear pair. Once this is accomplished, the load-distribution factor may be calculated.

In some cases it may not be possible to fully define or even estimate the value of  $e_t$ . In such cases an empirical approach may be used. We discuss both approaches in some detail.

The empirical approach requires only minimal data, and so it is the simplest to apply. Several conditions must be met, however, prior to using this method:

1. Net face width to pinion pitch diameter ratios must be less than or equal to 2.0. (For double-helix gears, the gap is not included in the face width.)
2. The gear elements are mounted between bearings (not overhung).
3. Face width can be up to 40 in.
4. There must be contact across the full face width of the narrowest member when loaded.
5. Gears are not highly crowned.

The empirical expression for the load-distribution factor is

$$C_m = K_m = 1.0 + C_{mc}(C_{pf}C_{pm} + C_{ma}C_e) \tag{10.21}$$

- where  $C_{mc}$  = lead correction factor
- $C_{pf}$  = pinion proportion factor
- $C_{pm}$  = pinion proportion modifier
- $C_{ma}$  = mesh alignment factor
- $C_e$  = mesh alignment correction factor

The lead correction factor  $C_{mc}$  modifies the peak loading in the presence of slight crowning or lead correction as follows:

$$C_{mc} = \begin{cases} 1.0 & \text{for gear with unmodified leads} \\ 0.8 & \text{for gear with leads properly modified by crowning or lead correction} \end{cases}$$

Figure 10.8 shows the pinion proportion factor  $C_{pf}$ , which accounts for deflections due to load. The pinion proportion modifier  $C_{pm}$  alters  $C_{pf}$  based on the location of the pinion relative to the supporting bearings. Figure 10.9 defines the factors  $S$  and  $S_1$ . And  $C_{pm}$  is defined as follows:

$$C_{pm} = \begin{cases} 1.0 & \text{when } S_1/S < 0.175 \\ 1.1 & \text{when } S_1/S \geq 0.175 \end{cases}$$

The mesh alignment factor  $C_{ma}$  accounts for factors other than elastic deformations. Figure 10.10 provides values for this factor for four accuracy groupings. For double-helix gears, this figure should be used with  $F$  equal to half of the total face width. The mesh alignment correction factor  $C_e$  modifies the mesh alignment factor to allow for the improved alignment which may be obtained when a gear set is adjusted at assembly or when the gears are modified by grinding, skiving, or lapping to more closely match their mates at assembly (in which case, pinion and gear

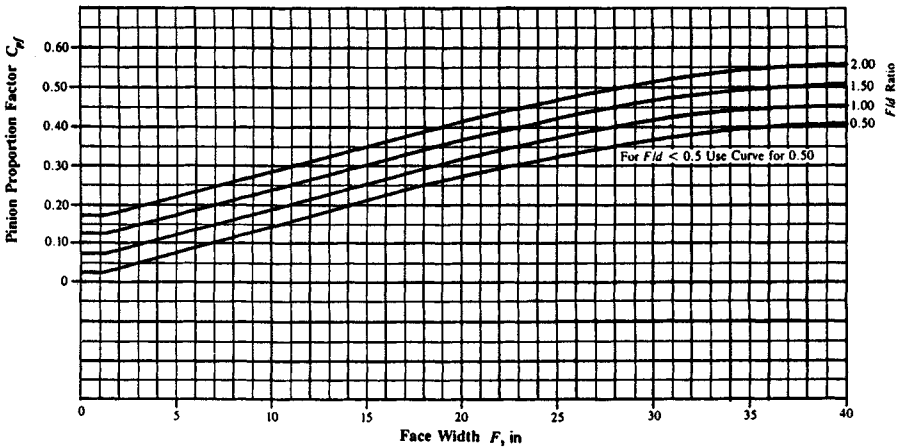


FIGURE 10.8 Pinion proportion factor  $C_{pf}$  (From Ref. [10.1].)

become a matched set). Only two values are permissible for  $C_e$ —either 1.0 or 0.8, as defined by the following requirements:

$$C_e = \begin{cases} 0.80 & \text{when the compatibility of the gearing is improved by lapping, grinding, or skiving after trial assembly to improve contact} \\ 0.80 & \text{when gearing is adjusted at assembly by shimming support bearings and/or housing to yield uniform contact} \\ 1.0 & \text{for all other conditions} \end{cases}$$

If enough detailed information is available, a better estimate of the load-distribution factor may be obtained by using a more analytical approach. This method, however, requires that the total alignment error  $e_t$  be calculated or estimated. Depending on the contact conditions, one of two expressions is used to calculate the load-distribution factor.

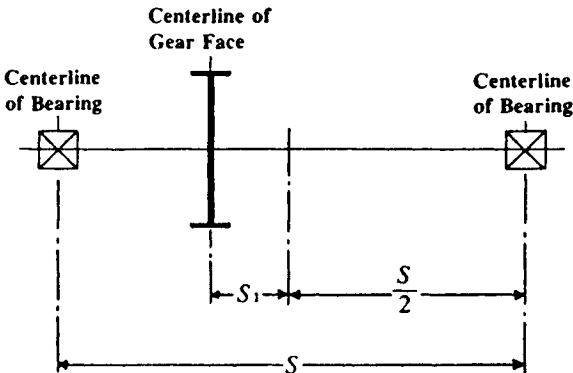
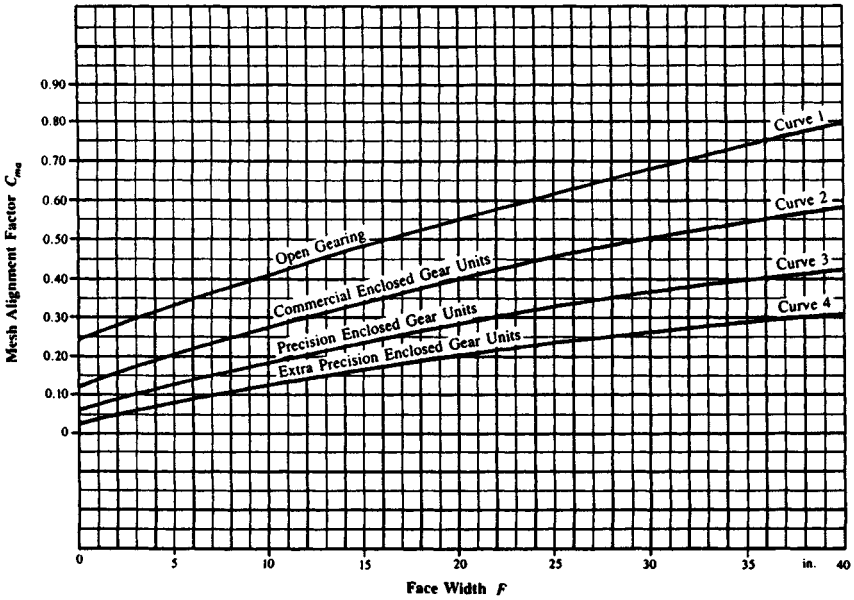


FIGURE 10.9 Definition of distances  $S$  and  $S_1$ . Bearing span is distance  $S$ ; pinion offset from midspan is  $S_1$ . (From Ref. [10.1].)



**FIGURE 10.10** Mesh alignment factor  $C_{ma}$ . For analytical method for determination of  $C_{ma}$ , see Eq. (10.21). (From Ref. [10.1].)

If the tooth contact pattern at normal operating load essentially covers the entire available tooth face, Eq. (10.22) should be used. If the tooth contact pattern does not cover the entire available tooth face (as would be the case for poorly aligned or high-crowned gears) at normal operating loads, then Eq. (10.23) must be used:

$$C_m = 1.0 + \frac{G_e Z F}{4W_t p_b} \tag{10.22}$$

and

$$C_m = \sqrt{\frac{G_e Z F}{W_t p_b}} \tag{10.23}$$

- where  $W_t$  = tangential tooth load, pounds (lb)
- $G$  = tooth stiffness constant, (lb/in)/in of face
- $Z$  = length of line of contact in transverse plane
- $e_t$  = total effective alignment error, in/in
- $p_b$  = transverse base pitch, in
- $F$  = net face width of narrowest member, in

The value of  $G$  will vary with tooth proportions, tooth thickness, and material. For steel gears of standard or close to standard proportions, it is normally in the range of  $1.5 \times 10^6$  to  $2.0 \times 10^6$  psi. The higher value should be used for higher-pressure-angle teeth, which are normally stiffer, while the lower value is representative of more flexible teeth. The most conservative approach is to use the higher value in all cases.

For double-helix gears, each half should be analyzed separately by using the appropriate values of  $F$  and  $e_t$  and by assuming that half of the tangential tooth load is transmitted by each half (the values for  $p_b$ ,  $Z$ , and  $G$  remain unchanged).

**Geometry Factor I.** The geometry factor  $I$  evaluates the radii of curvature of the contacting tooth profiles based on the pressure angle, helix, and gear ratio. Effects of modified tooth proportions and load sharing are considered. The  $I$  factor is defined as follows:

$$I = \frac{C_c C_x C_\psi^2}{m_N} \quad (10.24)$$

where  $C_c$  = curvature factor at operating pitch line  
 $C_x$  = contact height factor  
 $C_\psi$  = helical overlap factor  
 $m_N$  = load-sharing ratio

The curvature factor is

$$C_c = \frac{\cos \phi_o \sin \phi_o}{2} \frac{N_G}{N_G + N_P} \quad (10.25)$$

for external mesh; for internal mesh,

$$C_c = \frac{\cos \phi_o \sin \phi_o}{2} \frac{N_G}{N_G - N_P} \quad (10.26)$$

The contact height factor  $C_x$  adjusts the location on the tooth profile at which the critical contact stress occurs (i.e., face-contact ratio  $> 1.0$ ). The stress is calculated at the mean diameter or the middle of the tooth profile. For low-contact-ratio helical gears (that is, face-contact ratio  $\leq 1.0$ ), the stress is calculated at the lowest point of single-tooth contact in the transverse plane and  $C_x$  is given by Eq. (10.27):

$$C_x = \frac{R_1 R_2}{R_P R_G} \quad (10.27)$$

where  $R_P$  = pinion curvature radius at operating pitch point, in  
 $R_G$  = gear curvature radius at operating pitch point, in  
 $R_1$  = pinion curvature radius at critical contact point, in  
 $R_2$  = gear curvature radius at critical contact point, in

The required radii are given by

$$R_P = \frac{d}{2} \sin \phi_o \quad R_G = \frac{D}{2} \sin \phi_o \quad (10.28)$$

where  $d$  = pinion operating pitch diameter, in  
 $D$  = gear operating pitch diameter, in  
 $\phi_o$  = operating pressure angle in transverse plane, deg

$$R_1 = R_P - Z_c \quad (10.29)$$

and

$$R_2 = R_G + Z_c \quad (10.30)$$

for external gears; for internal gears,

$$R_2 = R_G - Z_c \quad (10.31)$$

where  $Z_c$  is the distance along the line of action in the transverse plane to the critical contact point. The value of  $Z_c$  is dependent on the transverse contact ratio. For helical gears where the face-contact ratio  $\leq 1.0$ ,  $Z_c$  is found by using Eq. (10.32). For normal helical gears where the face-contact ratio is  $> 1.0$ , Eq. (10.33) is used:

$$Z_c = p_b - 0.5[(d_o^2 - d_b^2)^{1/2} - (d^2 - d_b^2)^{1/2}] \quad m_F \leq 1.0 \quad (10.32)$$

and

$$Z_c = 0.5 [(d^2 - d_b^2)^{1/2} - (d_m^2 - d_b^2)^{1/2}] \quad m_F > 1.0 \quad (10.33)$$

where  $p_b$  = base pitch, in  
 $d_o$  = pinion outside diameter, in  
 $d_b$  = pinion base diameter, in  
 $d_m$  = pinion mean diameter, in

The pinion mean diameter is defined by Eq. (10.34) or (10.35). For external mesh,

$$d_m = C_o - \frac{D_o - d_o}{2} \quad (10.34)$$

For internal mesh,

$$d_m = \frac{D_I + d_o}{2} - C_o \quad (10.35)$$

where  $D_o$  = external gear outside diameter and  $D_I$  = internal gear inside diameter.

The helical factor  $C_\psi$  accounts for the partial helical overlap action which occurs in helical gears with a face-contact ratio  $m_F \leq 1.0$ . For helical gears with a face-contact ratio  $> 1.0$ ,  $C_\psi$  is set equal to unity; for low-contact helical gears, it is

$$C_\psi = \sqrt{1 - m_F + \frac{C_{xn} Z m_F^2}{C_x F \sin \psi_b}} \quad (10.36)$$

where  $Z$  = total length of line of action in transverse plane, in  
 $F$  = net minimum face width, in  
 $m_F$  = face-contact ratio  
 $C_x$  = contact height factor [Eq. (10.27)]  
 $C_{xn}$  = contact height factor for equivalent normal helical gears [Eq. (10.37)]  
 $\psi_b$  = base helix angle, deg

The  $C_{xn}$  factor is given by

$$C_{xn} = \frac{R_{1n} R_{2n}}{R_P R_G} \quad (10.37)$$

where  $R_{1n}$  = curvature radius at critical point for equivalent normal helical pinion, in  
 $R_{2n}$  = curvature radius at critical contact point for equivalent normal helical gear, in

The curvature radii are given by

$$R_{1n} = R_P - Z_c \quad (10.38)$$

$$R_{2n} = R_G + Z \quad \text{external gears} \quad (10.39)$$

$$R_{2n} = R_G - Z_c \quad \text{internal gears}$$

where Eq. (10.38) applies to external gears and Eq. (10.39) to either, as appropriate. Also, the term  $Z_c$  is obtained from Eq. (10.32).

The load-sharing ratio  $m_N$  is the ratio of the face width to the minimum total length of the contact lines:

$$m_N = \frac{F}{L_{\min}} \quad (10.40)$$

where  $m_N$  = load-sharing ratio

$F$  = minimum net face width, in

$L_{\min}$  = minimum total length of contact lines, in

The calculation of  $L_{\min}$  is a rather involved process. For most helical gears which have a face-contact ratio of at least 2.0, a conservative approximation for the load-sharing ratio  $m_N$  may be obtained from

$$m_N = \frac{P_N}{0.95Z} \quad (10.41)$$

where  $p_N$  = normal circular pitch in inches and  $Z$  = length of line of action in the transverse plane in inches. For helical gears with a face-contact ratio of less than 2.0, it is imperative that the actual value of  $L_{\min}$  be calculated and used in Eq. (10.40). The method for doing this is shown in Eqs. (10.42) through (10.45):

$$L_{\min} = \frac{1}{\sin \psi_b} [(P_1 - Q_1) + (P_2 - Q_2) + \dots + (P_i - Q_i) + \dots + (P_n - Q_n)] \quad (10.42)$$

where  $n$  = limiting number of lines of contact, as given by

$$n = \frac{(Z/\tan \psi_b) + F}{p_x} \quad (10.43)$$

Also,  $P_i$  = sum of base pitches in inches. The  $i$ th term of  $P_i$  is the lesser of

$$ip_x \tan \psi_b \quad \text{or} \quad Z \quad (10.44)$$

Finally,  $Q_i$  = remainder of base pitches in inches. Its value is

$$Q_i = 0 \quad \text{if } ip_x \leq F$$

But when  $ip_x > F$ , then  $Q_i$  is the  $i$ th term and is the lesser of

$$(ip_x - F) \tan \psi_b \quad \text{or} \quad Z \quad (10.45)$$

**Geometry Factor J.** The bending strength geometry factor is

$$J = \frac{YC_{\psi}}{K_f m_N} \tag{10.46}$$

- where  $Y$  = tooth form factor
- $K_f$  = stress correction factor
- $C_{\psi}$  = helical factor
- $m_N$  = load-distribution factor

The helical and load-distribution factors were both defined in the discussion of the geometry factor  $I$ . The calculation of  $Y$  is also a long, tedious process. For helical gears in which load sharing exists among the teeth in contact and for which the face-contact ratio is at least 2.0, the value of  $Y$  need not be calculated, since the value for  $J$  may be obtained directly from the charts shown in Figs. 10.11 through 10.25 with Eq. (10.47):

$$J = J' Q_{TR} Q_{TT} Q_A Q_H \tag{10.47}$$

- where  $J'$  = basic geometry factor
- $Q_{TR}$  = tool radius adjustment factor
- $Q_{TT}$  = tooth thickness adjustment factor
- $Q_A$  = addendum adjustment factor
- $Q_H$  = helix-angle adjustment factor

In using these charts, note that the values of addendum, dedendum, and tool-tip radius are given for a 1-normal-pitch gear. Values for any other pitch may be obtained by dividing the factor by the actual normal diametral pitch. For example, if an 8-normal-pitch gear is being considered, the parameters shown on Fig. 10.11 are

$$\text{Addendum } a = \frac{1.0}{8} = 0.125 \text{ in}$$

$$\text{Dedendum } b = \frac{1.35}{8} = 0.16875 \text{ in}$$

$$\text{Tool (hob) tip radius } r_T = \frac{0.42}{8} = 0.0525 \text{ in}$$

The basic geometry factor  $J'$  is found from Figs. 10.11 through 10.25. The tool radius adjustment factor  $Q_{TR}$  is found from Figs. 10.14 through 10.16 if the edge radius on the tool is other than  $0.42/P_d$ , which is the standard value used in calculating  $J'$ . Similarly, for gears with addenda other than  $1.0/P_d$  or tooth thicknesses other than the standard value of  $\pi/(2P_d)$ , the appropriate factors may be obtained from these charts. In the case of a helical gear, the adjustment factor  $Q_H$  is obtained from Figs. 10.23 through 10.25. If a standard helical gear is being considered,  $Q_{TR}$ ,  $Q_{TT}$ , and  $Q_A$  remain equal to unity, but  $Q_H$  must be found from Figs. 10.23 to 10.25.

These charts are computer-generated and, when properly used, produce quite accurate results. Note that they are also valid for spur gears if  $Q_H$  is set equal to unity (that is, enter Figs. 10.23 through 10.25 with  $0^\circ$  helix angle).

The charts shown in Figs. 10.11 through 10.25 assume the use of a standard full-radius hob. Additional charts, still under the assumption that the face-contact ratio is

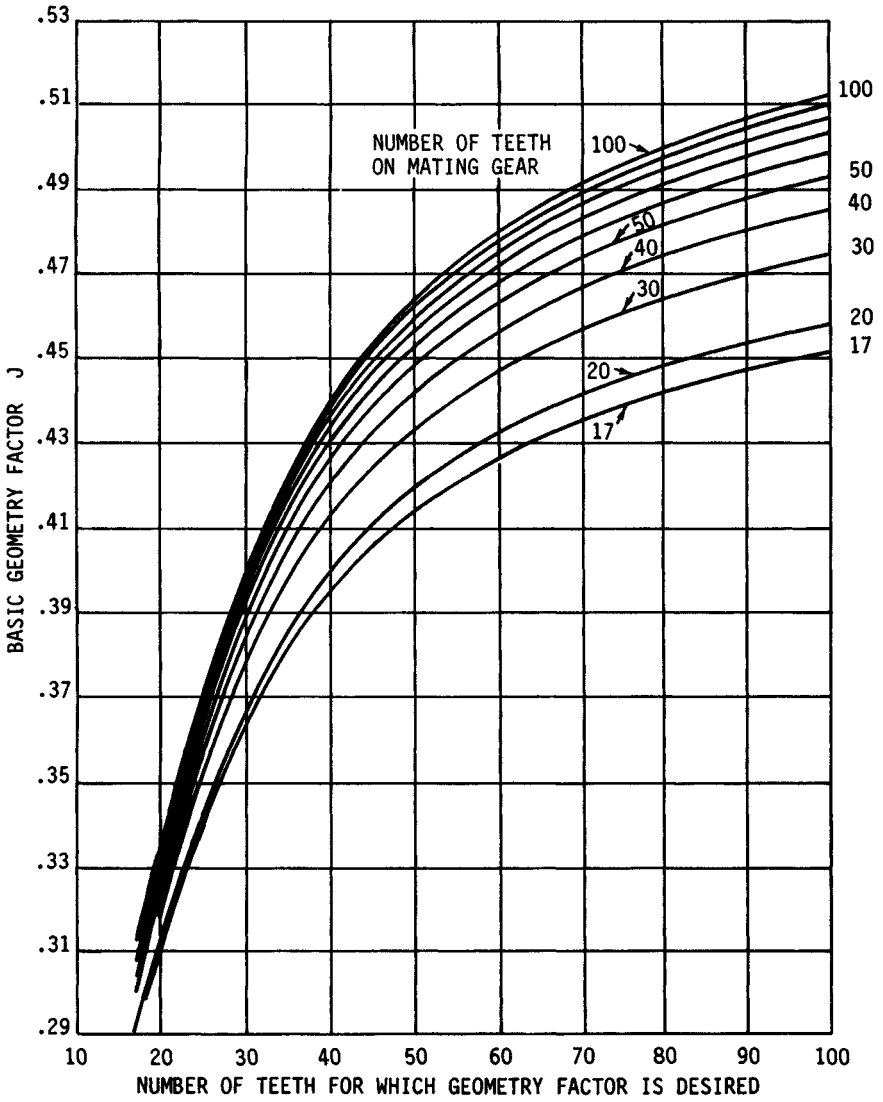
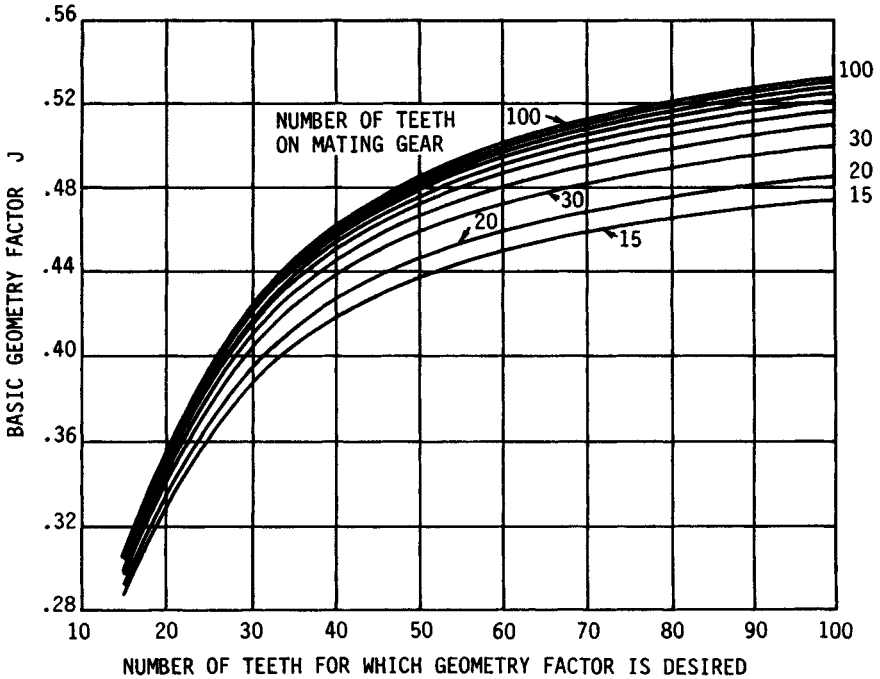


FIGURE 10.11 Basic geometry factors for 20° spur teeth;  $\phi_N = 20^\circ$ ,  $a = 1.00$ ,  $b = 1.35$ ,  $r_T = 0.42$ ,  $\Delta t = 0$ .



**FIGURE 10.12** Basic geometry factors for  $22\frac{1}{2}^\circ$  spur teeth;  $\phi_N = 22\frac{1}{2}^\circ$ ,  $a = 1.00$ ,  $b = 1.35$ ,  $r_T = 0.34$ ,  $\Delta t = 0$ .

at least 2.0 for other cutting-tool configurations, are shown in Figs. 10.26 through 10.36.<sup>†</sup> For these figures,

$$m_N = \frac{P_N}{0.95Z} \tag{10.48}$$

where the value of  $Z$  is for an element of indicated number of teeth and a 75-tooth mate. Also, the normal tooth thicknesses of pinion and gear teeth are each reduced 0.024 in, to provide 0.048 in of total backlash corresponding to a normal diametral pitch of unity. Note that these charts are limited to standard addendum, dedendum, and tooth thickness designs.

If the face-contact ratio is less than 2.0, the geometry factor must be calculated in accordance with Eq. (10.46); thus, it will be necessary to define  $Y$  and  $K_f$ . The definition of  $Y$  may be accomplished either by graphical layout or by a numerical iteration procedure. Since this Handbook is likely to be used by the machine designer with an occasional need for gear analysis, rather than by the gear specialist, we present the direct graphical technique. Readers interested in preparing computer codes or calculator routines might wish to consult Ref. [10.6].

The following graphical procedure is abstracted directly from Ref. [10.1] with permission of the publisher, as noted earlier. The  $Y$  factor is calculated with the aid

<sup>†</sup> These figures are extracted from AGMA 908-B89 with the permission of the AGMA.

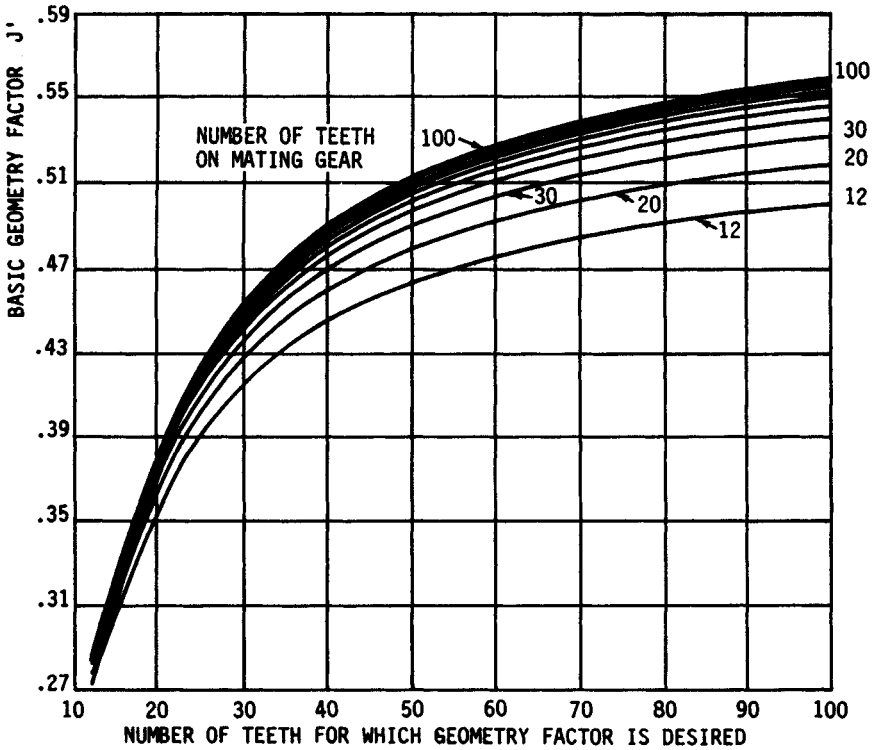


FIGURE 10.13 Basic geometry factors for 25° spur teeth;  $\phi_N = 25^\circ$ ,  $a = 1.00$ ,  $b = 1.35$ ,  $r_T = 0.24$ ,  $\Delta r = 0$ .

of dimensions obtained from an accurate layout of the tooth profile in the normal plane at a scale of 1 normal diametral pitch. Actually, any scale can be used, but the use of 1 normal diametral pitch is most convenient. Depending on the face-contact ratio, the load is considered to be applied at the highest point of single-tooth contact (HPSTC), Fig. 10.37, or at the tooth tip, Fig. 10.38. The equation is

$$Y = \frac{K_\psi P_s}{[\cos(\phi_L)/\cos(\phi_{No})][(1.5/uc_h) - \tan(\phi_L)/t]} \quad (10.49)$$

The terms in Eq. (10.49) are defined as follows:

$K_\psi$  = helix-angle factor

$\phi_{No}$  = normal operating pressure angle [Eq. (10.14)]

$\phi_L$  = load angle

$C_h$  = helical factor

$t$  = tooth thickness from layout, in

$u$  = radial distance from layout, in

$P_s$  = normal diametral pitch of layout (scale pitch), usually  $1.0 \text{ in}^{-1}$

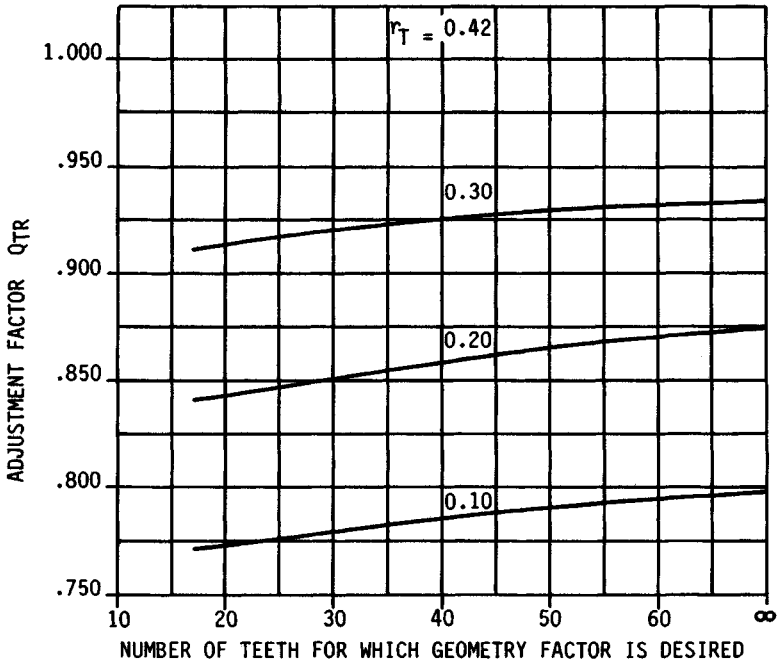


FIGURE 10.14 Tool-tip radius adjustment factor for 20° spur teeth. Tool-tip radius =  $r_T$  for a 1-diametral-pitch gear.

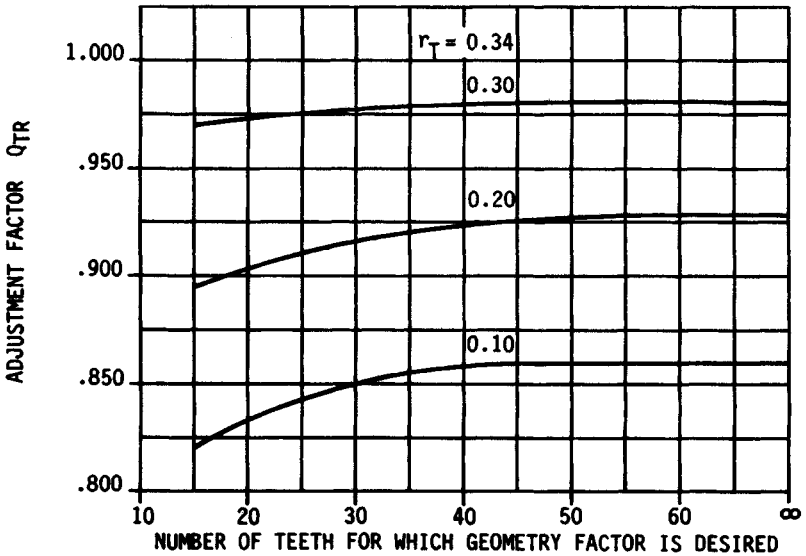


FIGURE 10.15 Tool-tip radius adjustment factor for 22½° spur teeth. Tool-tip radius =  $r_T$  for a 1-diametral-pitch gear.

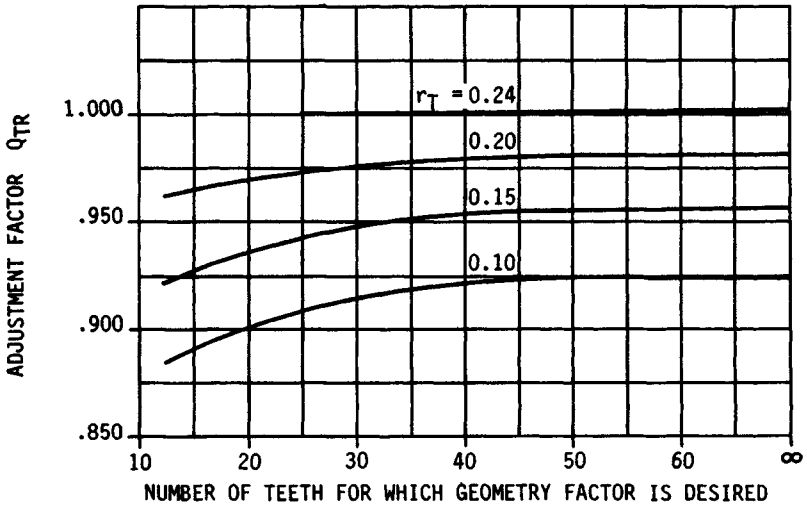


FIGURE 10.16 Tool-tip radius adjustment factor for 25° spur teeth. Tool-tip radius =  $r_T$  for a 1-diametral-pitch gear.

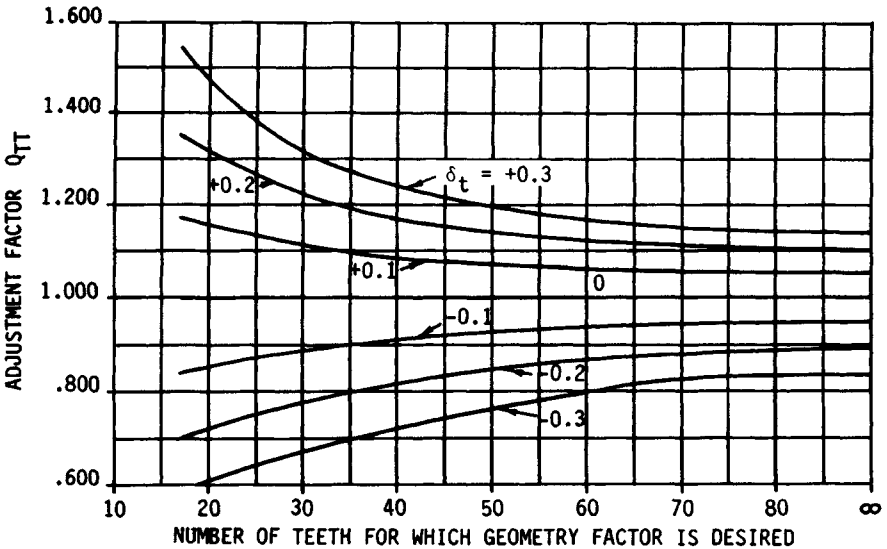
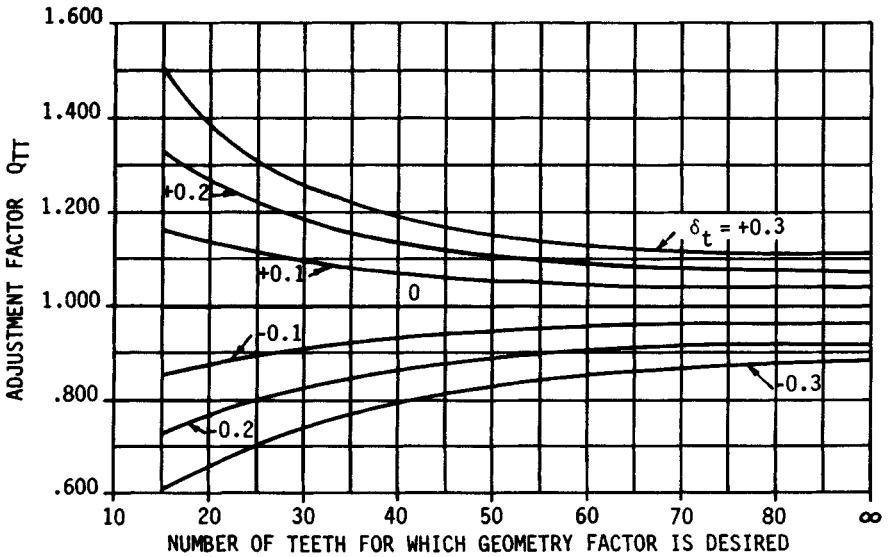
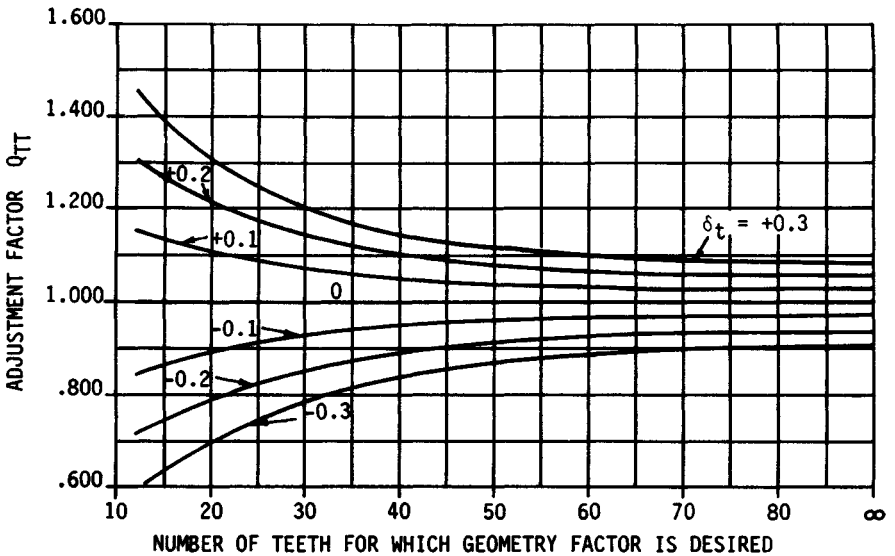


FIGURE 10.17 Tooth thickness adjustment factor  $Q_{TT}$  for 20° spur teeth. Tooth thickness modification =  $\delta_t$  for 1-diametral-pitch gears.



**FIGURE 10.18** Tooth thickness adjustment factor  $Q_{TT}$  for 22½° spur teeth. Tooth thickness modification =  $\delta_t$ , for 1-diametral-pitch gears.



**FIGURE 10.19** Tooth thickness adjustment factor  $Q_{TT}$  for 25° spur teeth. Tooth thickness modification =  $\delta_t$ , for 1-diametral-pitch gears.

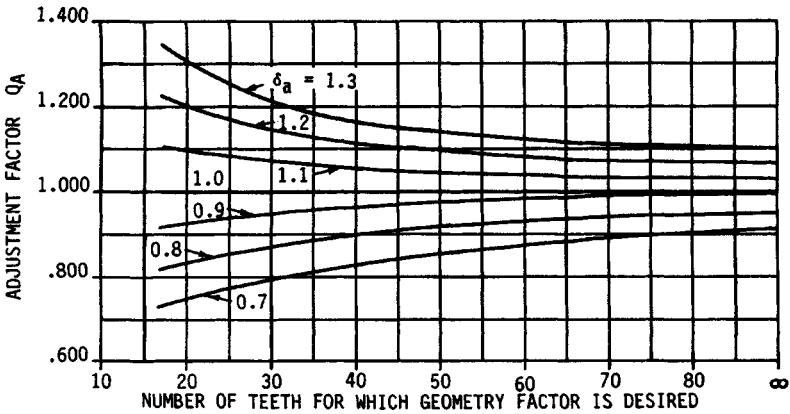


**FIGURE 10.20** Addendum adjustment factor  $Q_A$  for  $20^\circ$  spur teeth. Addendum factor modification =  $\delta_a$  for 1-diametral-pitch gears.

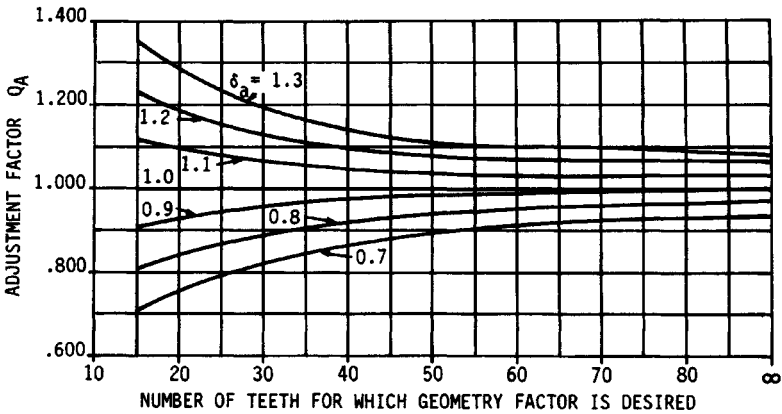


**FIGURE 10.21** Addendum adjustment factor  $Q_A$  for  $22\frac{1}{2}^\circ$  spur teeth. Addendum factor modification =  $\delta_a$  for 1-diametral-pitch gears.

To make the Y factor layout for a helical gear, an equivalent normal-plane gear tooth must be created, as follows:

$$N_e = \frac{N_p}{\cos^3 \psi} \tag{10.50}$$

$$d_c = \frac{dP_{nd}}{\cos^2 \psi} \tag{10.51}$$

$$d_{be} = d_e \cos \phi_n = N_e \cos \phi_c \tag{10.52}$$

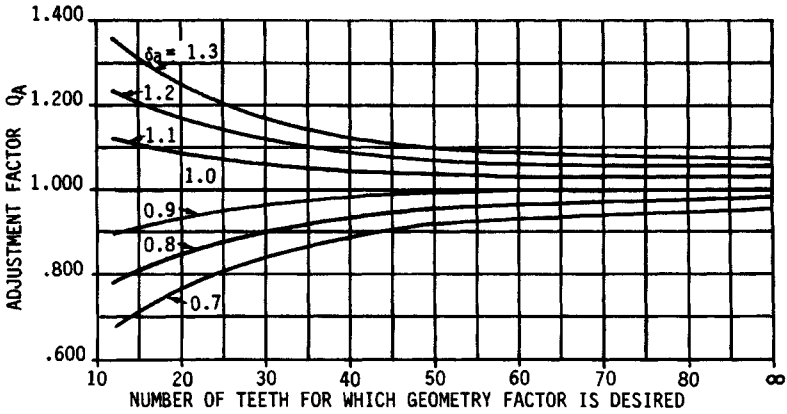


**FIGURE 10.22** Addendum adjustment factor  $Q_A$  for 25° spur teeth. Addendum factor modification =  $\delta_a$  for 1-diametral-pitch gears.

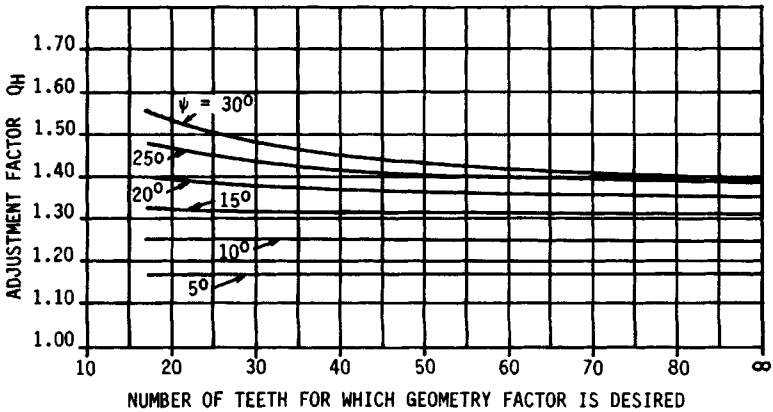


**FIGURE 10.23** Helix-angle adjustment factor  $Q_H$  for  $\phi_N = 20^\circ$ .

$$a = \frac{d_o - d}{2} P_{nd} \tag{10.53}$$

$$b = \frac{d - d_R}{2} P_{nd} \tag{10.54}$$

$$d_{oe} = d_e + 2a \tag{10.55}$$

$$d_{Re} = d_e - 2b \tag{10.56}$$

$$r_1 = \frac{(b - r_{Te})^2}{R_o + b - r_{Te}} \tag{10.57}$$

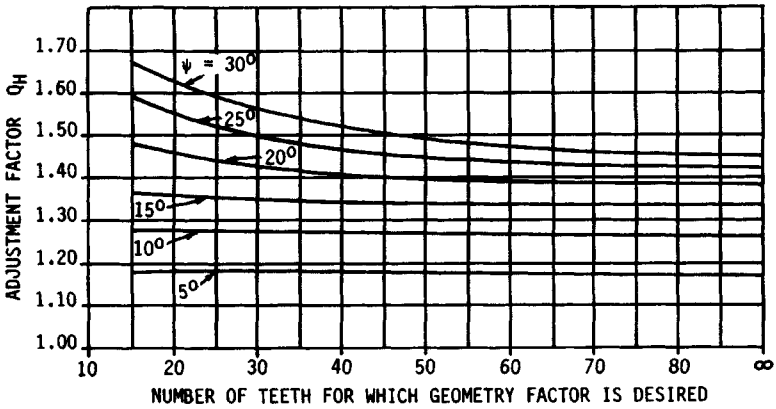


FIGURE 10.24 Helix-angle adjustment factor  $Q_H$  for  $\phi_N = 22\frac{1}{2}^\circ$ .

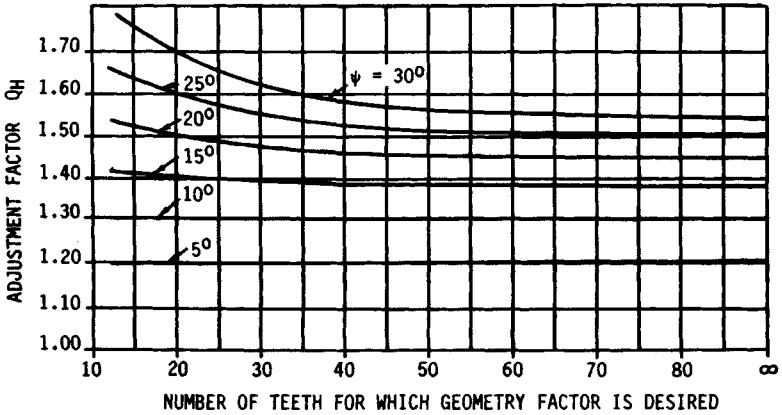


FIGURE 10.25 Helix-angle adjustment factor  $Q_H$  for  $\phi_N = 25^\circ$ .

$$r_f = r_1 + r_{Te} \tag{10.58}$$

$$r_{Te} = r_T P_{nd} \tag{10.59}$$

For a hob or rack-shaped cutting tool,

$$R_o = \frac{d_{se}}{2} \tag{10.60}$$

For a pinion-shaped cutting tool,

$$R_o = \frac{d_{se} D_c P_{nd}}{2(d_{se} + D_c P_{nd})} \tag{10.61}$$

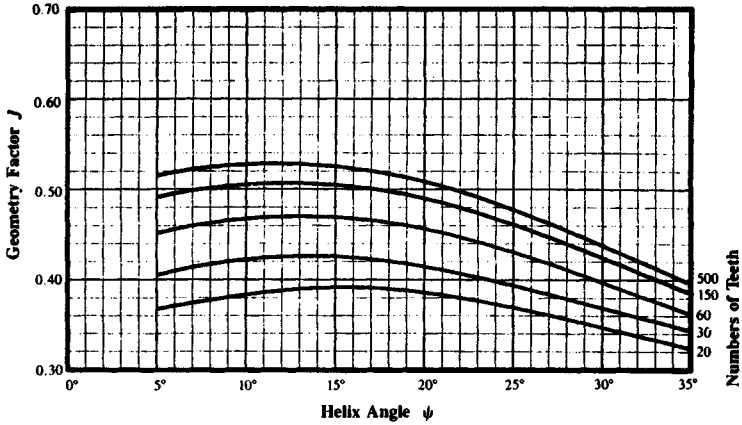


**FIGURE 10.26** Geometry factor  $J$  for a  $14\frac{1}{2}^\circ$  normal-pressure-angle helical gear. These factors are for a standard addendum finishing hob as the final machining operation. See Fig. 10.27a. (From AGMA 908-B89.)

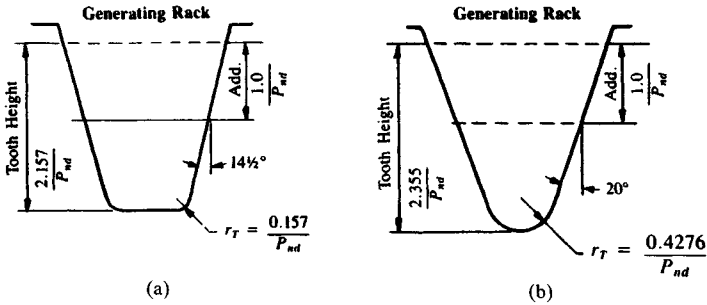


**FIGURE 10.27** Generating racks. (a) For teeth of Fig. 10.26; (b) for teeth of Fig. 10.29. (From AGMA 218.01.)

$$D_e = \frac{DP_{nd}}{\cos^2 \psi} \tag{10.62}$$

$$A = \frac{D_o - D}{2} P_{nd} \tag{10.63}$$

$$D_{oe} = D_e + 2A \tag{10.64}$$

$$D_{be} = D_e \cos \phi_n \tag{10.65}$$

$$d_{se} = \frac{N_e}{P_s} \tag{10.66}$$

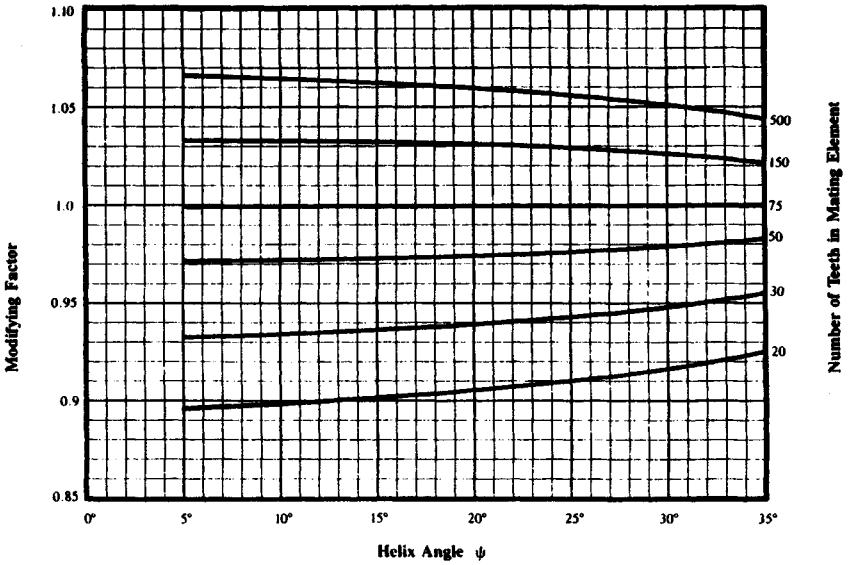


**FIGURE 10.28** *J* factor multipliers for 14½° normal-pressure-angle helical gear. These factors can be applied to the *J* factor when other than 75 teeth are used in the mating element. (From AGMA 908-B89.)

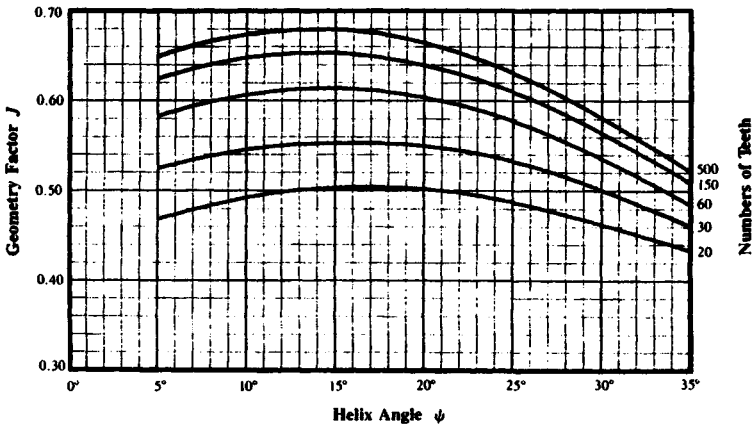


**FIGURE 10.29** Geometry factor *J* for a 20° normal-pressure-angle helical gear. These factors are for standard addendum teeth cut with a full-fillet hob. See Fig. 10.27*b*. (From AGMA 908-B89.)

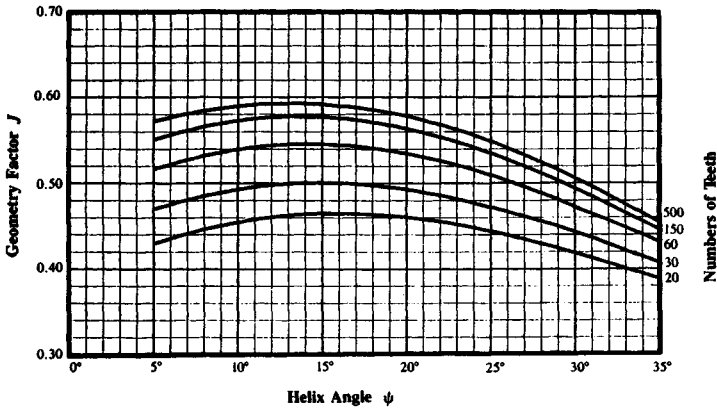


**FIGURE 10.30** Geometry factor  $J$  for a  $20^\circ$  normal-pressure-angle helical gear. These factors are for standard addendum teeth cut with a finishing hob as the final machining operation. See Fig. 10.31a. (From AGMA 908-B89.)

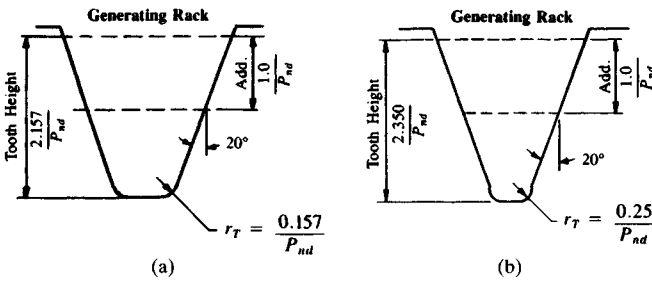


**FIGURE 10.31** Generating racks. (a) For teeth of Fig. 10.30; (b) for teeth of Fig. 10.32. (From AGMA 908-B89.)

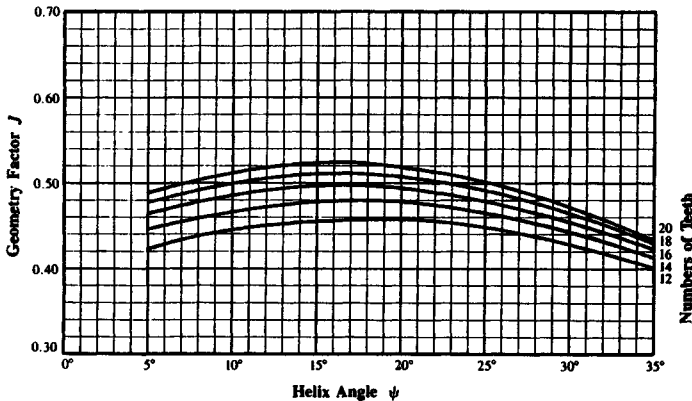


**FIGURE 10.32** Geometry factor  $J$  for  $20^\circ$  normal-pressure-angle helical gear. These factors are for long-addendum (125 percent of standard) shaved teeth cut with a preshave hob. See Fig. 10.31b. (From AGMA 908-B89.)

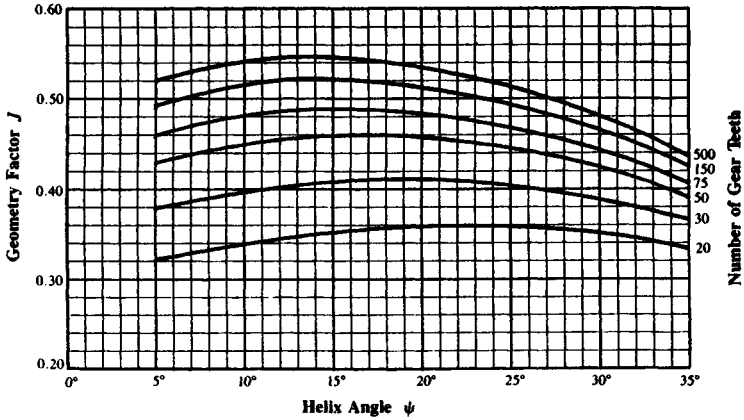


**FIGURE 10.33** Geometry factor  $J$  for  $20^\circ$  normal-pressure-angle helical gear. These factors are for short-addendum teeth (75 percent of standard) cut with a preshawe hob. See Fig. 10.34. (From AGMA 908-B89.)

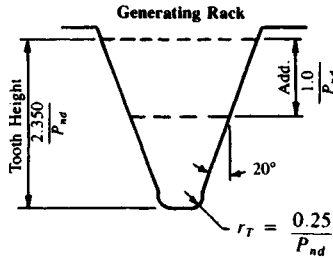


**FIGURE 10.34** Generating rack for teeth of Fig. 10.33. (From AGMA 908-B89.)

- where
- $N_e$  = equivalent number of pinion teeth
  - $d_{ve}$  = equivalent generating pitch diameter, in
  - $d_R$  = root diameter for actual number of teeth and generated pitch, in
  - $d_{Re}$  = equivalent root diameter for equivalent number of teeth, in
  - $d_{be}$  = equivalent base diameter for equivalent number of teeth, in
  - $d_e$  = equivalent operating pitch diameter for equivalent number of teeth, in
  - $d_{oe}$  = equivalent outside diameter for equivalent number of teeth, in
  - $a$  = operating addendum of pinion at 1 normal diametral pitch, in
  - $b$  = operating dedendum of pinion at 1 normal diametral pitch, in
  - $r_f$  = minimum fillet radius at root circle of layout, in
  - $r_T$  = edge radius of cutting tool, in
  - $r_{Te}$  = equivalent edge radius of cutting tool, in
  - $R_o$  = relative radius of curvature of pitch circle of pinion and pitch line or circle of cutting tool, in
  - $D_c$  = pitch diameter of pinion-shaped cutting tool, in
  - $D_e$  = equivalent operating pitch diameter of mating gear for equivalent number of teeth, in

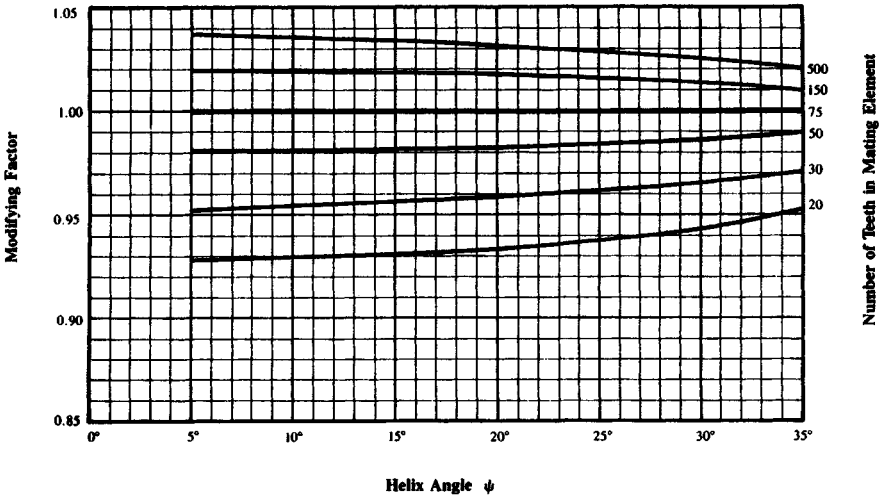


**FIGURE 10.35**  $J$  factor multipliers for 20° normal-pressure-angle helical gears. These factors can be applied to the  $J$  factor when other than 75 teeth are used in the mating element. (From Ref. [10.1].)

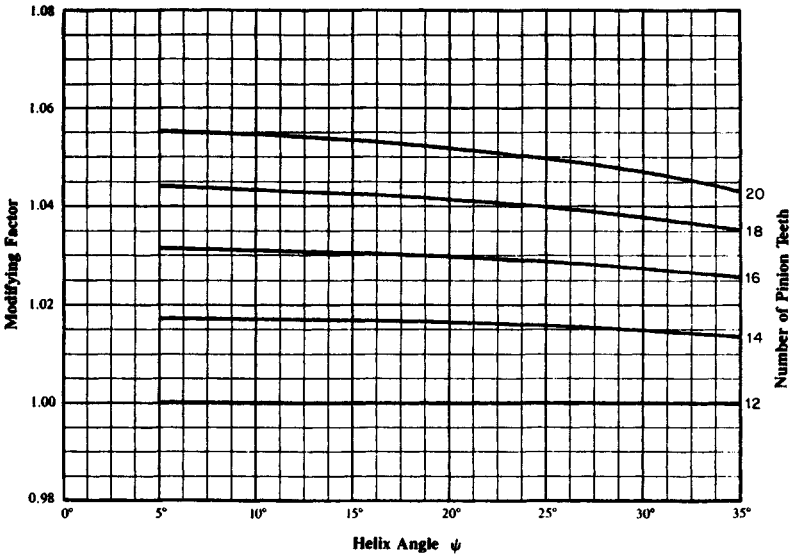


**FIGURE 10.36**  $J$  factor multipliers for 20° normal-pressure-angle helical gears with short addendum (75 percent of standard). These factors can be applied to the  $J$  factor when other than 75 teeth are used in the mating element. (From Ref. [10.1].)

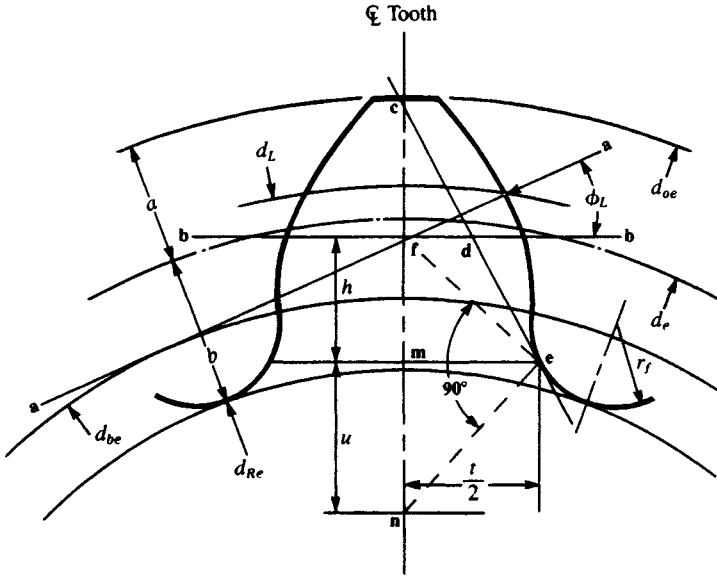


**FIGURE 10.37** Tooth form factor with load at highest point of single-tooth contact (HPSTC) shown in the normal plane through the pitch point. Note that  $r_f$  occurs at the point where the trochoid meets the root radius. (From Ref. [10.1].)

- $D_{oe}$  = equivalent outside diameter of mating gear for equivalent number of teeth, in
- $D_{be}$  = equivalent base diameter of mating gear for equivalent number of teeth, in
- $A$  = operating addendum of mating gear at 1 normal diametral pitch, in

The dimensions defined by Eqs. (10.50) through (10.66) are then used to make a tooth-stress layout, as shown in either Fig. 10.37 or 10.38 as required by the face-contact ratio. That is, helical gears with low face-contact ratio ( $m_F \leq 1.0$ ) are assumed to be loaded at the highest point of single-tooth contact; normal helical gears ( $m_F > 1.0$ ) use tip loading, and the  $C_h$  factor compensates for the actual loading on the oblique line.

To find  $Y$  from the above data, a graphical construction, as follows, is required. For low-contact-ratio helical gears (with  $m_F \leq 1.0$ ), using Fig. 10.37, draw a line  $\bar{a}\bar{a}$  through point  $p$ , the intersection of diameter  $d_L$  with the profile, and tangent to the base diameter  $d_{be}$ :

$$d_L = 2 \left\{ \left[ \sqrt{\left(\frac{d_e}{2}\right)^2 - \left(\frac{d_{be}}{2}\right)^2} + Z_d \right]^2 + \left(\frac{d_{be}}{2}\right)^2 \right\}^{1/2} \tag{10.67}$$

where  $Z_d$  = distance on line of action from highest point of single-tooth contact to pinion operating pitch circle, in inches, and so

$$Z_d = \pi \cos \phi_c - Z_e \tag{10.68}$$

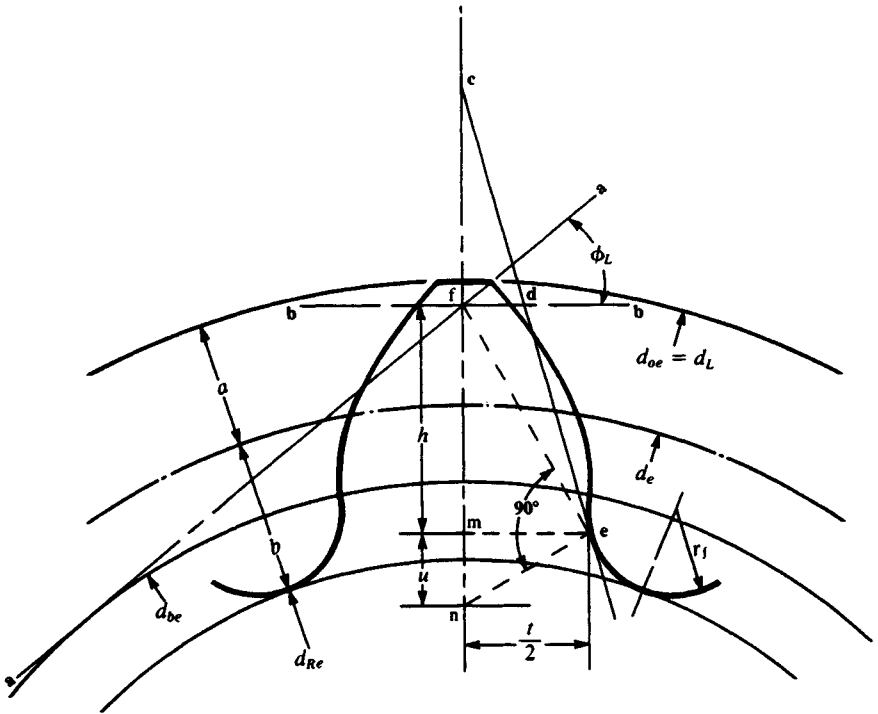


**FIGURE 10.38** Tooth form factor layout with load at tooth tip; shown in normal plane through the pitch point. (From Ref. [10.1].)

Letting  $Z_e$  = distance on line of action from gear outside diameter to pinion operating pitch circle, in inches, we have

$$Z_e = \sqrt{\left(\frac{D_{oe}}{2}\right)^2 - \left(\frac{D_{be}}{2}\right)^2} - \sqrt{\left(\frac{D_e}{2}\right)^2 - \left(\frac{D_{be}}{2}\right)^2} \quad (10.69)$$

For normal helical gears with  $m_F > 1.0$ , using Fig. 10.38, we find  $D_L = d_{oe}$ . Draw a line  $\bar{a}\bar{a}$  through point  $p$ , the tip of the tooth profile, and tangent to the base diameter  $d_{be}$ . Continue the layout for all gear types as follows:

Through point  $f$ , draw a line  $\bar{b}\bar{b}$  perpendicular to the tooth centerline. The included angle between lines  $\bar{a}\bar{a}$  and  $\bar{b}\bar{b}$  is load angle  $\phi_L$ .

Draw line  $\bar{c}\bar{d}\bar{e}$  tangent to the tooth fillet radius  $r_f$  at  $e$ , intersecting line  $\bar{b}\bar{b}$  at  $d$  and the tooth centerline at  $c$  so that  $\bar{c}\bar{d} = \bar{d}\bar{e}$ .

Draw line  $\bar{f}\bar{e}$ .

Through point  $e$ , draw a line perpendicular to  $\bar{f}\bar{e}$ , intersecting the tooth centerline at  $n$ .

Through point  $e$ , draw a line  $\bar{m}\bar{e}$  perpendicular to the tooth centerline.

Measure the following in inches from the tooth layout:

$$\bar{m}\bar{n} = u \quad \bar{m}\bar{e} = \frac{t}{2}$$

and

$$\overline{mf} = h \quad (\text{required for calculating } K_f)$$

The helix-angle factor  $K_\psi$  is set equal to unity for helical gears with  $m_F \leq 1.0$ , but for helical gears with  $m_F > 1.0$ , it is given by

$$K_\psi = \cos \psi_o \cos \psi \quad (10.70)$$

where  $\psi_o$  = helix angle at operating pitch diameter [from Eq. (10.13)] and  $\psi$  = helix angle at standard pitch diameter.

The helical factor  $C_h$  is the ratio of the root bending moment produced by the same intensity of loading applied along the actual oblique contact line (Fig. 10.39). If the face width of one gear is substantially larger than that of its mate, then full buttressing may exist on the wider face gear. If one face is wider than its mate by at least one addendum on both sides, then the value of  $C_h$  defined below may be increased by 10 percent only. The helical factor is given by either Eq. (10.71) for low-contact-ratio helical gears ( $m_F \leq 1.0$ ) or Eq. (10.72) for normal-contact-ratio ( $m_F > 1.0$ ) helicals. These equations are valid only for helix angles up to 30°:

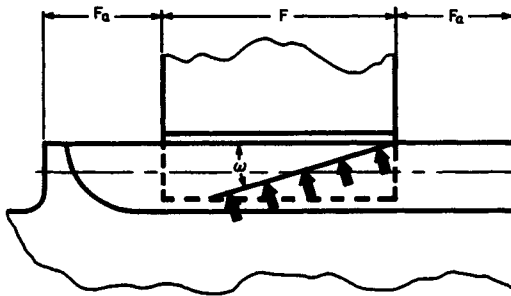


FIGURE 10.39 Oblique contact line. Full buttressing exists when  $F_a \geq$  one addendum.

$$C_h = 1.0 \quad (10.71)$$

$$C_h = \frac{1.0}{1 - [(\omega/100)(1 - \omega/100)]^{1/2}} \quad (10.72)$$

where  $\omega = \tan^{-1}(\tan \psi_o \sin \phi_{No})$  = inclination angle, deg  
 $\psi_o$  = helix angle at operating pitch diameter, deg [Eq. (10.13)]  
 $\phi_{No}$  = operating normal pressure angle, deg [Eq. (10.14)]

The tooth form factor  $Y$  may now be calculated from Eq. (10.49).

The stress correction factor is the last item which must be calculated prior to finding a value for the bending geometry factor  $J$ . Based on photoelastic studies by Dolan and Broghamer, the empirical relations shown in Eqs. (10.73) through (10.76) were developed:

$$K_f = H + \left(\frac{t}{r_f}\right)^L \left(\frac{t}{h}\right)^m \quad (10.73)$$

$$H = 0.18 - 0.008(\phi_{No} - 20) \tag{10.74}$$

$$L = H - 0.03 \tag{10.75}$$

$$m = 0.45 + 0.010(\phi_{No} - 20) \tag{10.76}$$

**Elastic Coefficient  $C_p$ .** This factor accounts for the elastic properties of various gear materials. It is given by Eq. (10.77). Table 10.4 provides values directly for  $C_p$  for various material combinations, for which Poisson's ratio is 0.30.

**TABLE 10.4** Values of Elastic Coefficient  $C_p$  for Helical Gears with Nonlocalized Contact and for  $\nu = 0.30$

Pinion material	Gear material					
	Steel	Malleable iron	Nodular iron	Cast iron	Aluminum bronze	Tin bronze
Steel, $E = 30\dagger$	2300	2180	2160	2100	1950	1900
Malleable iron, $E = 25$	2180	2090	2070	2020	1900	1850
Nodular iron, $E = 24$	2160	2070	2050	2000	1880	1830
Cast iron, $E = 22$	2100	2020	2000	1960	1850	1800
Aluminum bronze, $E = 17.5$	1950	1900	1880	1850	1750	1700
Tin bronze, $E = 16$	1900	1850	1830	1800	1700	1650

$\dagger$ Modulus of elasticity  $E$  is in megapounds per square inch (Mpsi).

$$C_p = \left\{ \frac{1}{\pi[(1 - \nu_p^2)/E_p + (1 - \nu_g^2)/E_g]} \right\}^{1/2} \tag{10.77}$$

where  $\nu_p, \nu_g$  = Poisson's ratio for pinion and gear, respectively  
 $E_p, E_g$  = modulus of elasticity for pinion and gear, respectively

**Allowable Stresses  $s_{ac}$  and  $s_{at}$ .** The allowable stresses depend on many factors, such as chemical composition, mechanical properties, residual stresses, hardness, heat treatment, and cleanliness. As a guide, the allowable stresses for helical gears may be obtained from Tables 10.5 and 10.6 or Figs. 10.40 and 10.41. Where a range of values is shown, the lowest values are used for general design. The upper values may be used only when the designer has certified that

1. High-quality material is used.
2. Section size and design allow maximum response to heat treatment.
3. Proper quality control is effected by adequate inspection.
4. Operating experience justifies their use.

Surface-hardened gear teeth require adequate case depth to resist the subsurface shear stresses developed by tooth contact loads and the tooth root fillet tensile stresses. But depths must not be so great as to result in brittle tooth tips and high residual tensile stress in the core.

**TABLE 10.5** Allowable Bending Stress Numbers  $s_m$  and Contact Stress Numbers  $s_{ac}$  for a Variety of Materials

AGMA class	Commercial designation	Heat treatment	Minimum hardness		$s_m$ , kpsi	$s_{ac}$ , kpsi	
			Surface	Core			
Steel							
A-1 through A-5		Through-hardened and tempered (Fig. 10-40)	180 $H_B$ and less		25-33	85-95	
			240 $H_B$		31-41	105-115	
			300 $H_B$		36-47	120-135	
			360 $H_B$		40-52	145-160	
			400 $H_B$		42-56	155-170	
			50-54 $R_C$		45-55	170-190	
			Flame- or induction-hardened† with type A pattern (Fig. 10-45)				
			Flame- or induction-hardened with type B pattern (Fig. 10-45)			22	
			Carburized† and case-hardened†	55 $R_C$		55-65	180-200
				60 $R_C$		55-70	200-225
	AISI 4140	Nitrided††	48 $R_C$	300 $H_B$	35-45	155-180	
	AISI 4340	Nitrided††	46 $R_C$	300 $H_B$	36-47	150-175	
	Nitalloy 135M	Nitrided††	60 $R_C$	300 $H_B$	38-48	170-195	
	2½% chrome	Nitrided††	54-60 $R_C$	350 $H_B$	55-65	155-216	

Cast iron						
20		As cast			5	50-60
30		As cast	175 $H_B$		8.5	65-75
40		As cast	200 $H_B$		13	75-85
Nodular (ductile) iron						
A-7-a	60-40-18	Annealed, quenched, and tempered	140 $H_B$		22-33	77-92
A-7-c	80-55-06		180 $H_B$		22-33	77-92
A-7-d	100-70-03		230 $H_B$		27-40	92-112
A-7-e	120-90-02		270 $H_B$		31-44	103-126
Malleable iron (pearlitic)						
A-8-c	45007		165 $H_B$		10	72
A-8-e	50005		180 $H_B$		13	78
A-8-f	53007		195 $H_B$		16	83
A-8-i	80002		240 $H_B$		21	94
Bronze						
Bronze 2	AGMA 2C	Sand-cast Sand-cast	Min. tensile strength 40 kpsi		5.7	30
Al/Br 3	ASTM B-148-52 Alloy 9C	Heat-treated	Min. tensile strength 90 kpsi		23.6	65

† The range of allowable stress numbers indicated corresponds to grade 1 and grade 2 steels. See tables 14-6 and 14-9 to 14-11 of source.

‡ The overload capacity of nitrided gears is low, since the shape of the effective SN curve is flat. The sensitivity to shock should be investigated before proceeding with the design.

SOURCE: Ref. [10.1].

**TABLE 10.6** Reliability Factors  $K_R$  and  $C_R$

Factor, $K_R$ or $C_R$	Probabilities, %	
	Success	Failure
1.50	99.99	0.01
1.25	99.90	0.10
1.00	99.00	1.00
0.85	90.00	10.00

The effective case depth for carburized and induction-hardened gears is defined as the depth below the surface at which the Rockwell C hardness has dropped to 50  $R_C$  or to 5 points below the surface hardness, whichever is lower.

The values and ranges shown in Fig. 10.42 have had a long history of successful use for carburized gears and can be used as guides. For gearing in which maximum performance is required, detailed studies must be made of the application, loading, and manufacturing procedures to obtain desirable gradients of both hardness and internal stress. Furthermore, the method of measuring the case, as well as the allowable tolerance in case depth, should be a matter of agreement between the customer and the manufacturer.

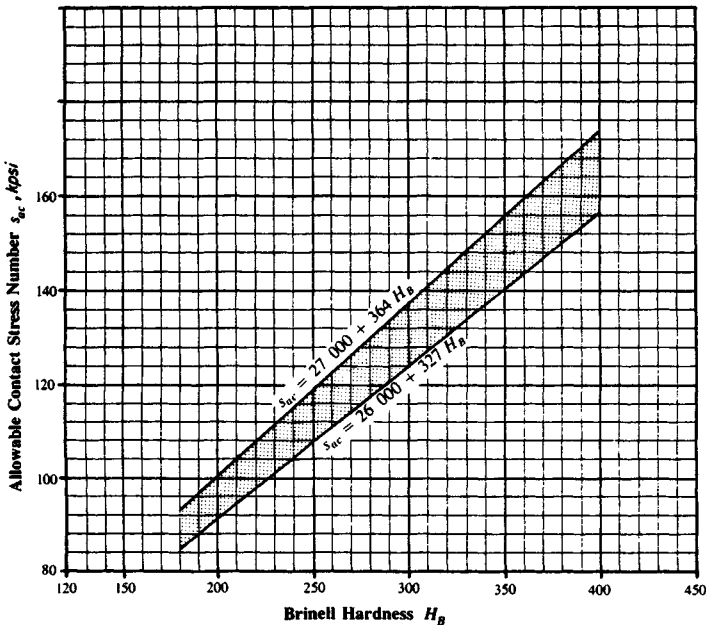


**FIGURE 10.40** Allowable contact stress number  $s_{ac}$  for steel gears. Lower curve is maximum for grade 1 and upper curve is maximum for grade 2. (From Ref. [10.1].)

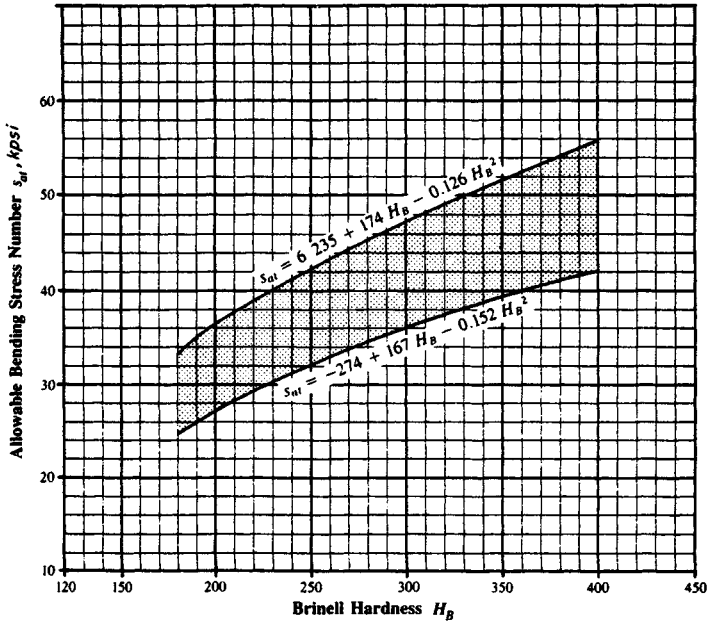


**FIGURE 10.41** Allowable bending stress number  $s_u$  for steel gears. Lower curve is maximum for grade 1 and upper curve is maximum for grade 2. (From Ref. [10.1].)

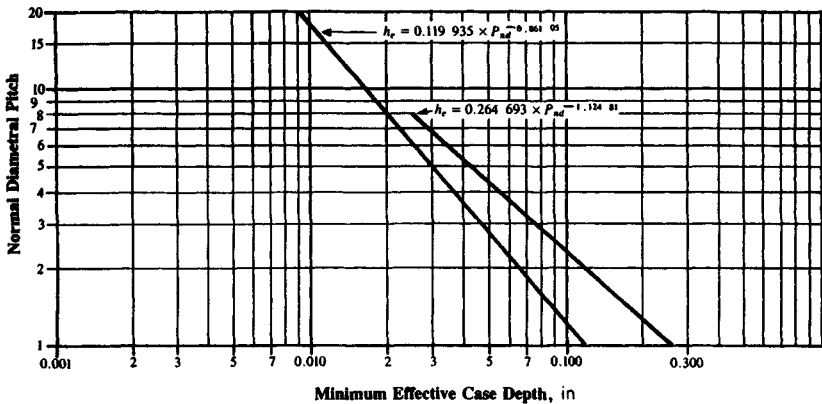


**FIGURE 10.42** Effective case depth  $h_c$  for carburized gears based on normal diametral pitch. The effective case depth is defined as the depth of case which has a minimum hardness of  $50 R_C$ . The total case depth to core carbon is about  $1.5h_c$ . The values and ranges shown on the case depth curves are to be used as guides. For gearing in which maximum performance is required, detailed studies must be made of the application, loading, and manufacturing procedures to obtain desirable gradients of both hardness and internal stress. Furthermore, the method of measuring the case as well as the allowable tolerance in case depth should be a matter of agreement between the customer and the manufacturer. (From Ref. [10.1].)

A guide for minimum effective case depth  $h_e$  at the pitch line for carburized and induction-hardened teeth, based on the depth of maximum shear from contact loading, is given by

$$h_e = \frac{C_G s_c d \sin \phi_o}{U_H \cos \psi_b} \quad (10.78)$$

where  $h_e$  = minimum effective case depth in inches and  $U_H$  = hardening process factor in pounds per square inch. In Eq. (10.78),  $U_H = 6.4 \times 10^6$  psi for carburized teeth and  $4.4 \times 10^6$  psi for tooth-to-tooth induction-hardened teeth.

You should take care when using Eq. (10.78) that adequate case depths prevail at the tooth root fillet, and that tooth tips are not overhardened and brittle. A suggested value of maximum effective case depth  $h_{e,max}$  at the pitch line is

$$h_{e,max} = \frac{0.4}{P_d} \quad \text{or} \quad h_{e,max} = 0.56t_o \quad (10.79)$$

where  $h_{e,max}$  = suggested maximum effective case depth in inches and  $t_o$  = normal tooth thickness at top land of gear in question, in inches.

For nitrided gears, case depth is specified as total case depth  $h_o$  and  $h_c$  is defined as the depth below the surface at which the hardness has dropped to 110 percent of the core hardness.

For gearing requiring maximum performance, especially large sizes, coarse pitches, and high contact stresses, detailed studies must be made of application, loading, and manufacturing procedures to determine the desirable gradients of hardness, strength, and internal residual stresses throughout the tooth.

A guide for minimum case depth for nitrided teeth, based on the depth of maximum shear from contact loading, is given by

$$h_c = \frac{C_G U_c s_c d \sin \phi_o}{(1.66 \times 10^7)(\cos \psi_b)} \quad (10.80)$$

where  $h_c$  = minimum total case depth in inches and  $U_c$  = core hardness coefficient, from Fig. 10.43.

If the value of  $h_c$  from Eq. (10.80) is less than the value from Fig. 10.44, then the minimum value from Fig. 10.44 should be used. The equation for the lower or left-hand curve in Fig. 10.44 is

$$h_c = (4.328\ 96)(10^{-2}) - P_{nd}(9.681\ 15)(10^{-3}) + P_{nd}^2(1.201\ 85)(10^{-3}) \\ - P_{nd}^3(6.797\ 21)(10^{-5}) + P_{nd}^4(1.371)(10^{-6}) \quad (10.81)$$

The equation of the right-hand curve is

$$h_c = (6.600\ 90)(10^{-2}) - P_{nd}(1.622\ 24)(10^{-2}) + P_{nd}^2(2.093\ 61)(10^{-3}) \\ - P_{nd}^3(1.177\ 55)(10^{-4}) + P_{nd}^4(2.331\ 60)(10^{-6}) \quad (10.82)$$

Note that other treatments of the subject of allowable gear-tooth bending recommend that the value obtained from Table 10.6 or Fig. 10.41 be multiplied by 0.70 for teeth subjected to reversed bending. This is not necessary within the context of this analysis, since the rim thickness factor  $K_b$  accounts for reversed bending.

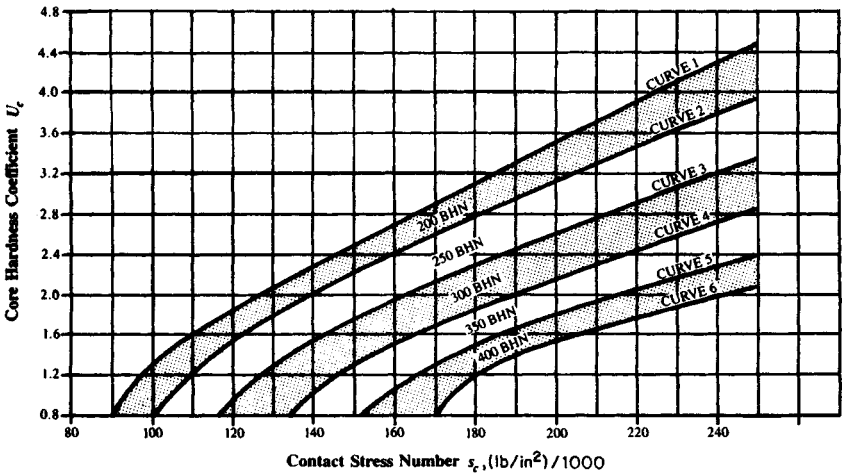


**FIGURE 10.43** Core-hardness coefficient  $U_c$  as a function of the contact stress number  $s_c$ . The upper portion of the core-hardness bands yields heavier case depths and is for general design purposes; use the lower portion of the bands for high-quality material. (From Ref. [10.1].)

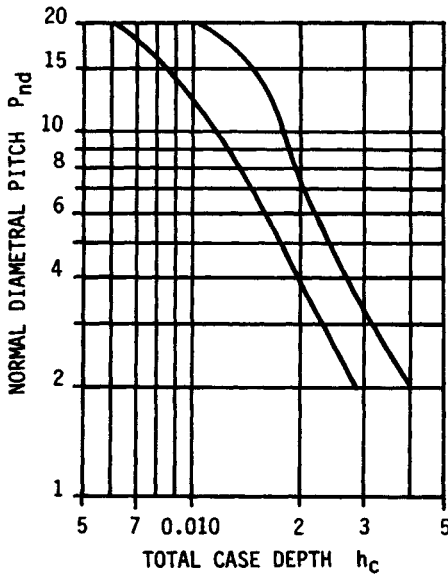
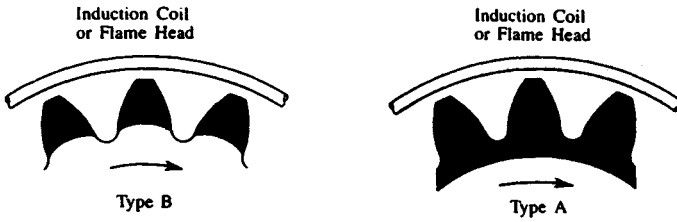


**FIGURE 10.44** Minimum total case depth  $h_c$  for nitrided gears based on the normal diametral pitch. (From Ref. [10.1].)

## Spin Hardening



## Flank Hardening

Inductor or Flame Head

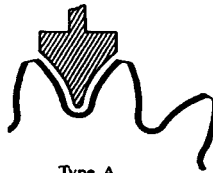


Type B

Inductor or Flame Head



Type B

Flank and Root Hardening  
Inductor or Flame Head

Type A

**FIGURE 10.45** Variations in hardening patterns obtainable with flame or induction hardening. (From Ref. [10.1].)

For through-hardened gears, the yield stress at maximum peak stress should also be checked as defined by Eq. (10.83):

$$S_{ay}K_y \geq \frac{W_{t,\max}K_a}{K_v} \frac{P_d}{F} \frac{K_m}{K_f} \quad (10.83)$$

where  $W_{t,\max}$  = peak tangential tooth load, lb

$K_a$  = application factor

$K_v$  = dynamic factor

$F$  = minimum net face width, in

$K_m$  = load-distribution factor

$K_f$  = stress correction factor

$K_y$  = yield strength factor

$S_{ay}$  = allowable yield strength number, psi (from Fig. 10.46)

The yield strength factor should be set equal to 0.50 for conservative practice or to 0.75 for general industrial use.

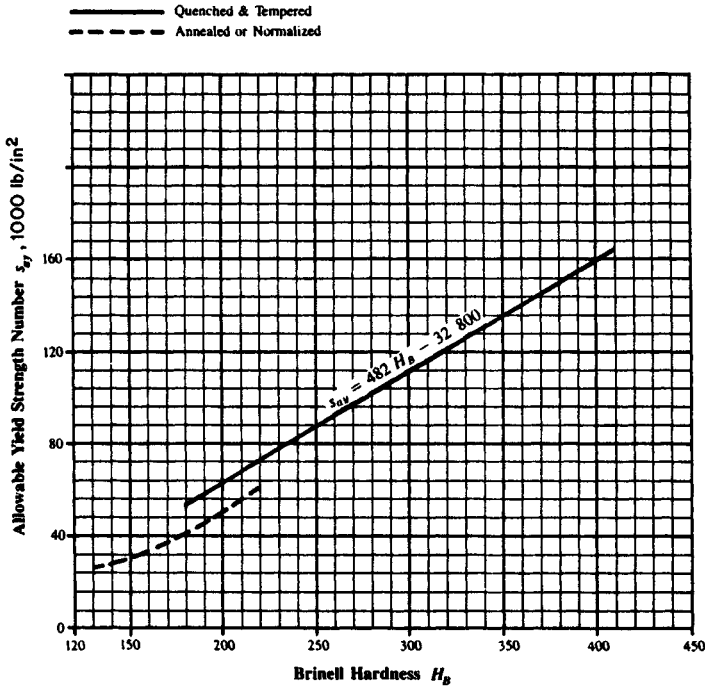


**FIGURE 10.46** Allowable yield strength number  $s_{ay}$  for steel gears. (From Ref. [10.1].)

**Hardness Ratio Factor  $C_H$ .** It is common practice in using through-hardened gear sets to utilize a higher hardness on the pinion than on the gear. The pinion typically sees many more cycles than the gear; thus a more economical overall design is obtained by balancing the surface durability and wear rate in this manner. Similarly, surface-hardened pinions may be used with through-hardened gears to provide improved overall capacity through the work-hardening effect which a “hard” pinion has on a “soft” gear. The hardness ratio factor adjusts the allowable stresses for this effect.

For through-hardened gear sets,  $C_H$  can be found from Fig. 10.47, while Fig. 10.48 provides values for surface-hardened pinions mating with through-hardened gears.

**Life Factors  $K_L$  and  $C_L$ .** The allowable stresses shown in Tables 10.5 and 10.6 and Figs. 10.40 and 10.41 are based on 10 000 000 load cycles. The life factor adjusts the allowable stresses for design lives other than 10 000 000 cycles. A unity value for the life factor may be used for design lives beyond 10 000 000 cycles only when it is justified by experience with similar designs.

Insufficient specific data are available to define life factors for most materials. For steel gears, however, experience has shown that the curves shown in Figs. 10.49 and 10.50 are valid.

In utilizing these charts, care should be exercised whenever the product of  $K_L$  and  $s_{at}$  equals or exceeds  $s_{ay}$ , as shown on Fig. 10.46, since this indicates that localized yielding may occur. For low-speed gears without critical noise vibration or transmis-

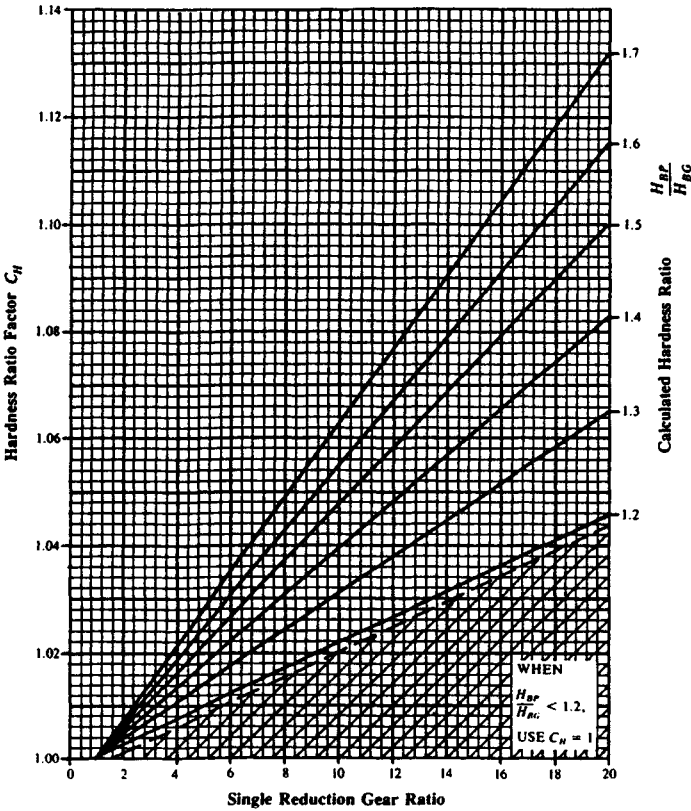


**FIGURE 10.47** Hardness ratio factor  $C_H$  for through-hardened gears. In this chart,  $H_{BP}$  is the Brinell hardness of the pinion, and  $H_{BG}$  is the Brinell hardness of the gear. (From Ref. [10.1].)

sion accuracy requirements, local yielding may be acceptable, but it should be avoided in general.

**Reliability Factors  $C_R$  and  $K_R$ .** The allowable stress levels are not absolute parameters. Rather, a specific probability of failure is associated with each allowable level. The values shown in Figs. 10.40 and 10.41 and Table 10.5 are based on a 99 percent probability of success (or a 1 percent probability of failure). This means that in a large population, at least 99 percent of the gears designed to a particular listed allowable stress will run for at least 10 000 000 cycles without experiencing a failure in the mode (that is, bending or durability) addressed.

In some cases it is desirable to design to higher or lower failure probabilities. Table 10.6 provides values for  $C_R$  and  $K_R$  which will permit the designer to do so. Before deciding on the reliability factor which is appropriate for a particular design, the analyst should consider what is meant by a "failure." In the case of a durability failure, a failure is said to have occurred when the first pit, or spall, is observed. Obviously a long time will elapse between the occurrence of a durability failure and the time at which the gear will cease to perform its normal power-transmission function.

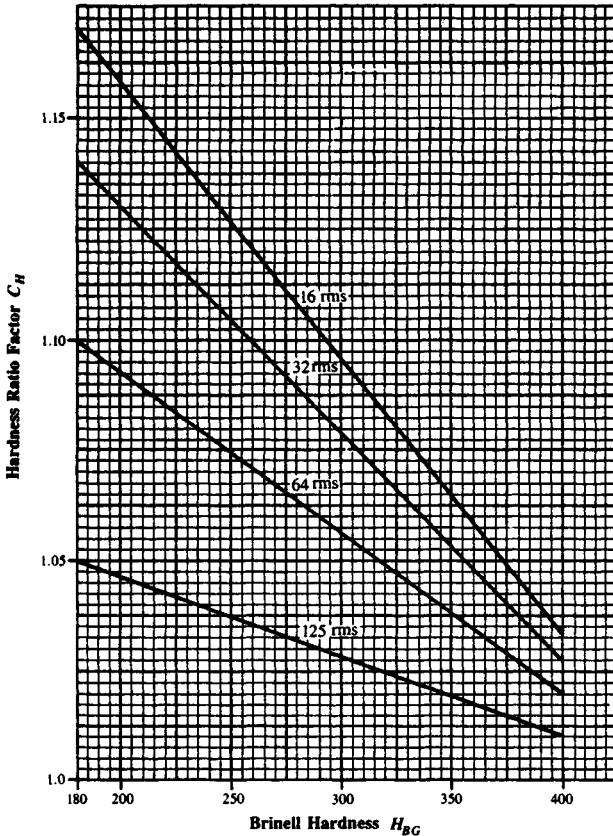


**FIGURE 10.48** Hardness ratio factor  $C_H$  for surface-hardened teeth. The rms values shown correspond to the surface finish of the pinion  $f_p$  in microinches. (From Ref. [10.1].)

In the case of a bending failure, the appearance of a crack in the fillet area is the criterion. In most cases, and for most materials, the progression of this crack to the point at which a tooth or a piece of tooth fractures is rather quick. A bending failure will almost always progress to the point where function is lost much more rapidly than a durability failure. For this reason it is sometimes desirable to use a higher value for  $K_R$  than for  $C_R$ .

Because of the load sharing which occurs on most normal helical gears, a complete fracture of a full single tooth, as often occurs on a spur gear, is not usually the mode of failure on a helical gear. A certain redundancy is built into a helical gear, since initially only a piece of a tooth will normally fracture.

**Temperature Factors  $C_T$  and  $K_T$ .** At gear blank operating temperatures below 250°F and above freezing, actual operating temperature has little effect on the allowable stress level for steel gears; thus a temperature factor of unity is used. At higher or lower temperatures, the allowable stress levels are altered considerably. Unfortunately, few hard data are available to define these effects. At very low tem-

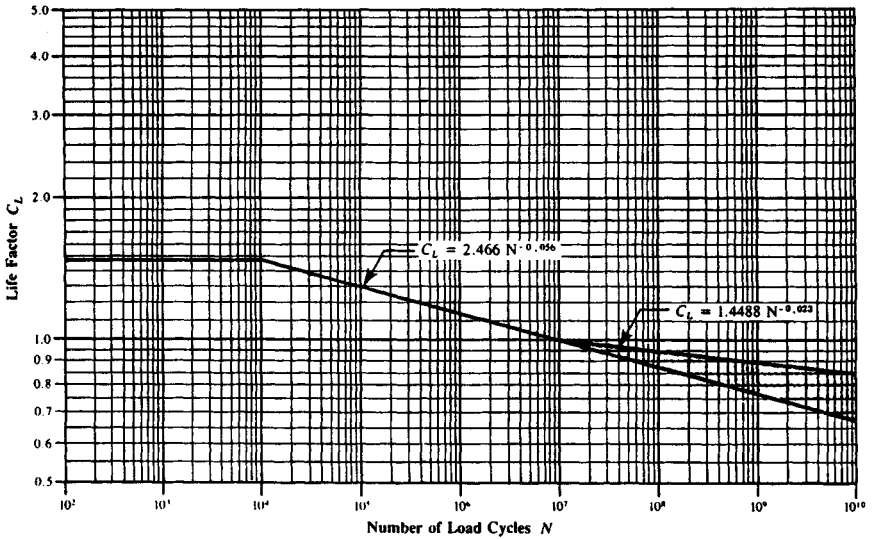


**FIGURE 10.49** Pitting-resistance life factor  $C_L$ . This curve does not apply where a service factor  $C_{SF}$  is used. *Note:* The choice of  $C_L$  above  $10^7$  cycles is influenced by lubrication regime, failure criteria, smoothness of operation required, pitch line velocity, gear material cleanliness, material ductility and fracture toughness, and residual stress. (From Ref. [10.1].)

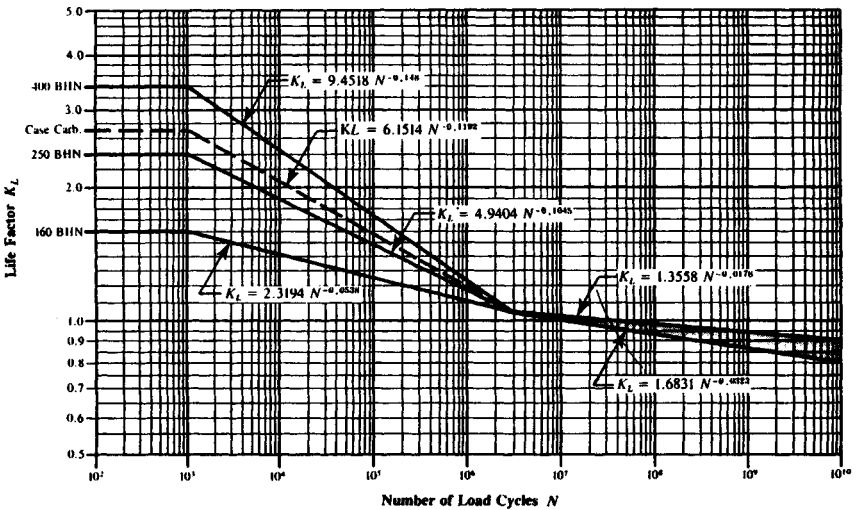


**FIGURE 10.50** Bending-strength life factor  $K_L$ . This chart does not apply where a service factor  $K_{SF}$  is used. *Note:* The choice of  $K_L$  above  $3 \times 10^6$  cycles is influenced by pitch line velocity, gear material cleanliness, residual stress, gear material ductility, and fracture toughness. (From Ref. [10.1].)

peratures, the impact resistance and fracture toughness of most materials are reduced; thus special care must be exercised in such designs if nonuniform loading is expected. A temperature factor greater than unity should be used in such cases. Although no specific data are available, a value between 1.25 and 1.50 is recommended for gears which must transmit full power between 0 and  $-50^{\circ}\text{F}$ .

At high temperatures, most materials experience a reduction in hardness level. Nonmetallic gears are not ordinarily used at high temperatures; thus our comments are restricted to steel gearing. The temperature factor should be chosen on the basis of the hot hardness curve for the particular material in use. That is, the temperature factor is equal to the allowable stress at room-temperature hardness divided by the allowable stress at the hardness corresponding to the higher temperature. For information related to typical trends, Fig. 10.51 shows the hardness-temperature characteristics for two gear steels (AISI 9310 and VASCO-X2). Two typical bearing steels (M-50 and SAE 52100) are also shown for reference purposes.

Once the strength and durability analyses have been completed, the wear and scoring resistance of the gears must be defined. Wear (see Chap. 34) is usually a concern only for relatively low-speed gears, whereas scoring is a concern only for relatively high-speed gears.

**Wear.** Gear-tooth wear is a very difficult phenomenon to predict analytically. Fortunately, it is not a major problem for most gear drives operating in the moderate- to

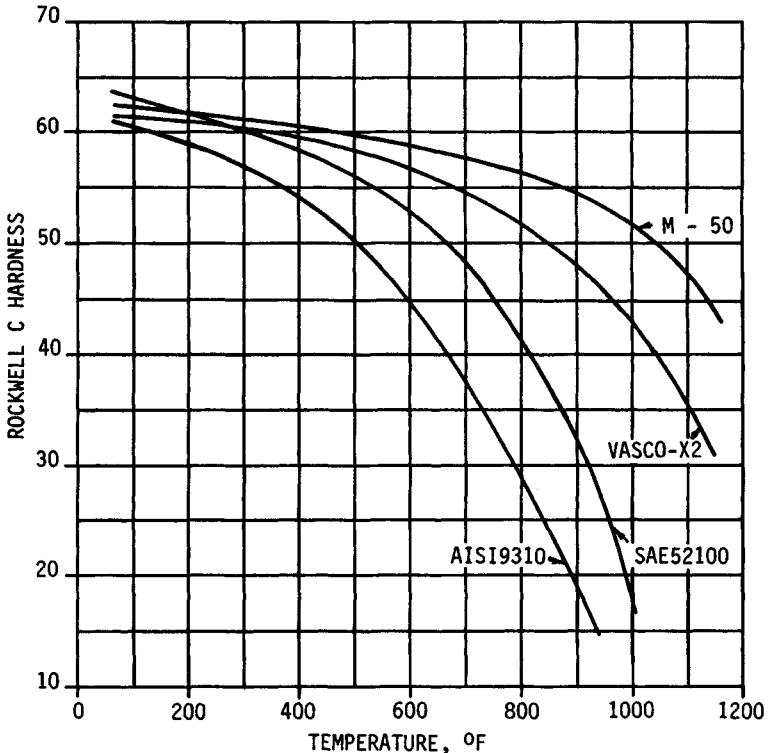


FIGURE 10.51 Hardness as a function of temperature for several steels.

high-speed range. In the case of low-speed gears, however, not only is wear a significant problem, but also it can be the limiting factor in defining the load capacity of the mesh.

In low-speed gear drives, the film which separates the mating tooth surfaces is insufficient to prevent metal-to-metal contact; thus wear occurs. In higher-speed gears, the film becomes somewhat thicker, and gross contact of the mating surfaces is prevented. Indeed, grinding lines are still visible on many aircraft gears after hundreds of hours of operation. The type of surface distress which will occur in a gear set is dependent, to a certain extent, on the pitch line velocity. As shown in Fig. 10.52, wear predominates in the lower-speed range, while scoring rules the upper-speed range. In the midrange, pitting controls the gear life.

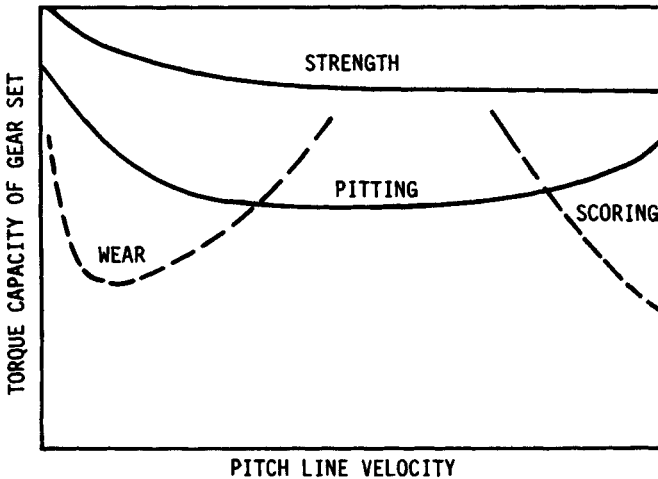


FIGURE 10.52 Gear distress as a function of pitch line velocity.

The elastohydrodynamic (EHD) film thickness can provide some guidance in the evaluation of the wear potential of a gear set. Care must be used in the application of these methods, since the existing data are far from complete and there are many instances of contradictory results. One of the simplest approaches is due to Dowson; see Ref. [10.7] and Chap. 20. The equation is

$$\frac{h}{R'} = \frac{(4.46 \times 10^{-5})(\alpha E')^{0.54} [\mu_o u / (E' R')]^{0.70}}{[w / (E' R')]^{0.13}} \quad (10.84)$$

where  $h$  = calculated minimum film thickness, in  
 $R'$  = relative radius of curvature in transverse plane at pitch point, in  
 $\alpha$  = lubricant pressure-viscosity coefficient, in<sup>2</sup>/lb  
 $E'$  = effective elastic modulus, psi  
 $\mu_o$  = sump lubricant viscosity, centipoise (cP)  
 $u$  = rolling velocity in transverse plane, inches per second (in/s)  
 $w$  = load per unit length of contact, lb/in

Wellauer and Holloway ([10.8]) present a nomograph to compute the film thickness at the pitch point; but this nomograph is quite detailed and is not included here.

The parameter of interest in our discussion is not the film thickness itself, but rather the ratio of the film thickness to the relative surface roughness. This ratio is defined as the *specific film thickness* and is given by

$$\lambda = \frac{h}{S'_r} \quad (10.85)$$

The relative surface roughness [root-mean-square (rms)] is given by

$$S'_r = \frac{S_P + S_G}{2} \quad (10.86)$$

Typical values for various gear manufacturing processes are shown in Table 10.7.

**TABLE 10.7** Tooth Surface Texture  
in the As-Finished Condition

Finish method	Surface texture in microinches (rms)	
	Range	Typical
Hobbed	30–80	50
Shaved	10–45	35
Lapped	20–200	93
Lapped and run in	20–100	53
Ground (soft)	5–35	25
Ground (hard)	5–35	15
Honed and polished	4–15	5

Once the specific film thickness has been determined, the probability of surface distress occurring can be determined through the use of Fig. 10.53.

Although the data presented thus far can be quite useful, several factors must be kept in mind in applying them to actual design. Most of the experimental data on which this information is based were obtained from through-hardened gear sets operating with petroleum-based oils. Gears operating with synthetic oils appear able to operate successfully at film thicknesses much less than those predicted by this analysis. The same is true for case-hardened gears of 59  $R_C$  and higher hardness. The results may be further altered by the use of friction modifiers or EP additives in the oil. Finally, wear, of and by itself, is not necessarily a failure. In many cases, wear is an acceptable condition; it is simply monitored until it reaches some predetermined level, at which time the gears are replaced.

Perhaps the most useful application for this analysis is as a comparative, relative rating tool, rather than as an absolute design criterion.

The occurrence of wear is difficult to predict, but the rate of wear is even more so. Equation (10.87) may be useful as a guide in predicting wear, but its accuracy has not been rigorously verified:

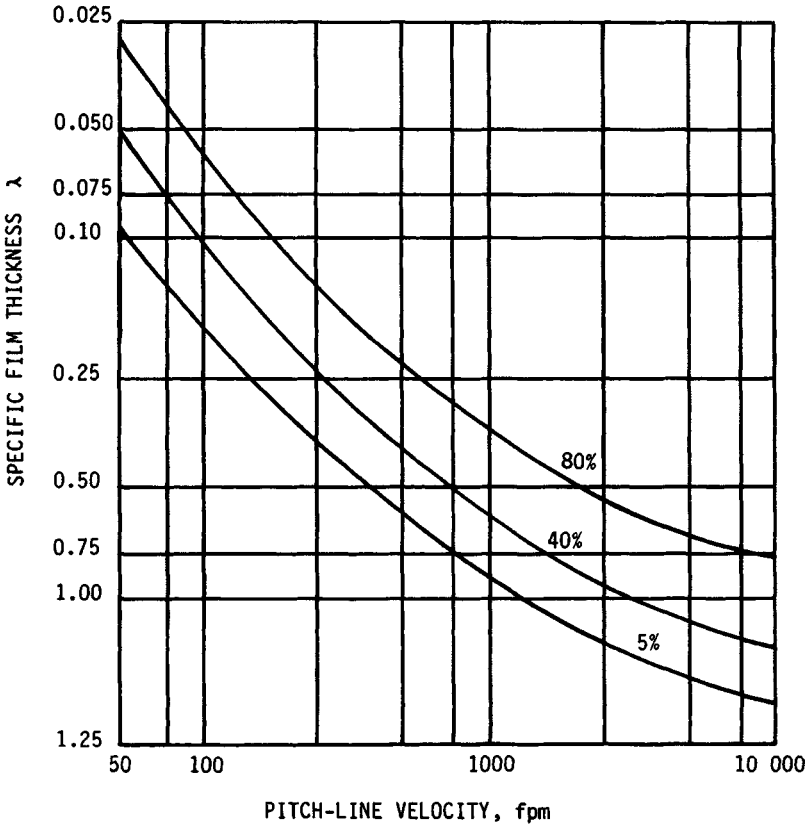


**FIGURE 10.53** Surface-distress probability chart as a function of pitch line velocity and specific film thickness. Curves represent 80, 40, and 5 percent probability of distress. The region above the 80 percent line is unsatisfactory; the region below the 5 percent line is good.

$$q = \frac{KW_t n_T}{FS_y} \tag{10.87}$$

where  $q$  = wear, in  
 $n_T$  = number of cycles  
 $S_y$  = yield strength of gear material, psi  
 $K$  = factor from Eq. (10.88)

and

$$3.1 \geq K\lambda^{1.645} \times 10^9 \geq 1.8 \tag{10.88}$$

In applying these equations, greater emphasis should be placed on the trend indicated than on the absolute value of the numbers. For example, a new design might be compared with an existing similar design for which the wear characteristics have been established. This could be accomplished by calculating the  $q$  value for each by

Eqs. (10.87) and (10.88) and then comparing them, rather than looking at absolute values of either. The ratio of the two  $q$  values is far more accurate than the absolute value of either.

**Scoring.** Very few data concerning the scoring behavior of gears are available in an easily usable form. Scoring is normally a problem for heavily loaded, high-speed steel gears. The exact mechanism by which scoring occurs is not yet fully understood.

At high speeds, the calculated film thickness is often quite large. Yet a wearlike failure mode sometimes occurs. Under high-speed conditions, the sliding motion of one gear tooth on another may create instantaneous conditions of temperature and pressure which destroy the film of oil separating the tooth flanks. When this occurs, the asperities on the surfaces of the mating teeth instantaneously weld. As the gears continue to rotate, these welds break and drag along the tooth flanks, causing scratches, or "score" marks, in the direction of sliding. If the damage which occurs is very slight, it is often referred to as *scuffing* or *frosting*. In some cases, light frosting may heal over and not progress; however, scoring is generally progressively destructive. Though never a catastrophic failure itself, scoring destroys the tooth surface, which leads to accelerated wear, pitting, and spalling. If scoring is allowed to progress unchecked, tooth fracture may ultimately occur.

Note that scoring is not a fatigue phenomenon; that is, its occurrence is not time-dependent. In general, if scoring does not occur within 15 to 25 minutes (min) at a certain operating condition, usually it will not occur *at that condition* at all. Only a change in operating condition, and not the accumulation of cycles, will cause scoring.

A theory known as the *critical-temperature theory*, originally proposed by Harmen Blok, is usually used in the evaluation of scoring hazard for a set of helical gears.

If we consider a simple analogy, the concept of critical temperature will become clear. Consider the old method of making fire by rubbing two sticks together. If the sticks are held together with only light pressure and/or they are rubbed slowly, they will simply wear. If, however, the pressure is increased and the sticks are rubbed more rapidly, then the temperature at the mating surfaces will increase. If the pressure (load) and the rubbing speed (sliding velocity) are progressively increased, eventually the sticks will ignite. At the point of ignition, the sticks have reached their *critical* temperature. Quite obviously, the critical temperature will vary with the type of wood, its moisture content, and other factors.

In a similar manner, as gear-tooth sliding velocity and load are increased, eventually a point will be reached at which the temperature at the conjunction attains a critical value, and then the film separating the tooth flanks will be destroyed. At this point the teeth are in metal-to-metal contact, and instantaneous welding of the surface asperities occurs. The continued rotation of the mesh rips apart these microscopic welds and produces the scored appearance from which this failure derives its name. The critical temperature varies with the type of gear material, surface hardness, surface finish, type and viscosity of oil, additives in the oil, etc. When the film is destroyed, it is sometimes referred to as *flashing*; thus the parameter used to evaluate this condition has come to be known as the *flash* temperature. When the flash temperature reaches its *critical* value, failure by scoring will occur. Note that the flash temperature referred to here is not related in any way to the flash point of the oil, and the oil flash point shown on some manufacturers' specification sheets is in no way related to the allowable flash temperature discussed here.

Many refinements have been made to Blok's original theory, and it is currently accepted as the best method available for evaluating scoring resistance for spur, helical, and bevel gears. Reference [10.9] presents a method of analysis for steel spur and

helical gears based on Blok's method. The scoring hazard is evaluated by calculating a flash temperature rise  $\Delta T_{Fi}$ . The flash temperature rise is added to the gear blank temperature  $T_B$  and compared with the allowable tooth flash temperature for the particular material and lubricant combination being used.

The flash temperature rise is given by

$$\Delta T_{Fi} = \left( \frac{W_i C_a C_m}{F C_v} \right)^{0.75} \left( \frac{n_p^{0.5}}{P_d^{0.25}} \right) (\mu Z_{ii}) \left( \frac{50}{50 - S'} \right) \quad (10.89)$$

where  $T_{Fi}$  = flash temperature rise at  $i$ th contact point along line of action, °F

$W_i$  = tangential tooth load at  $i$ th contact point, lb

$F$  = net minimum face width, in

$C_a$  = application factor

$C_m$  = load-distribution factor

$C_v$  = dynamic factor

$n_p$  = pinion speed, revolutions per minute (r/min)

$P_d$  = transverse diametral pitch

$S'$  = relative surface roughness, Eq. (10.86)

$Z_{ii}$  = scoring geometry factor at  $i$ th contact point along line of action

The factors  $C_w$ ,  $C_v$ , and  $C_m$  are the same as those used in the durability formula [Eq. (10.17)].

The scoring geometry factor is given by

$$Z_{ii} = \frac{0.2917[\rho_{Pi}^{1/2} - (N_p \rho_{Gi}/N_G)^{1/2}]P_d^{1/4}}{(\cos \phi_i)^{0.75}[\rho_{Pi} \rho_{Gi}/(\rho_{Pi} + \rho_{Gi})]^{0.25}} \quad (10.90)$$

where  $\rho_{Pi}$ ,  $\rho_{Gi}$  = radius of curvature of pinion and gear, respectively, at  $i$ th contact point, in

$N_p$ ,  $N_G$  = tooth numbers of pinion and gear, respectively

$P_d$  = transverse diametral pitch

$\phi_i$  = pressure angle at  $i$ th contact point, deg

The tooth flash temperature is then calculated by

$$T_{Fi} = T_B + \Delta T_{Fi} \quad (10.91)$$

**TABLE 10.8** Allowable Flash Temperatures for Some Gear Materials and for Spur and Helical Gears

The surface hardness is 60  $R_c$  for all materials listed.

Gear material	Oil type	Allowable flash temperature, °F
AISI 9310	MIL-L-7808	295
	MIL-L-23699	295
	XAS 2354	335†
VASCO-X2	MIL-L-7808	350
	MIL-L-23699	350
	XAS 2354	375†

†Conservative estimate based on limited current data.

In most cases the blank temperature will be very close to the oil inlet temperature. Thus, unless the actual blank temperature is known, the oil inlet temperature may be used for  $T_B$ . Table 10.8 gives allowable values of the total flash temperature.

Equations (10.89) through (10.91) refer to the  $i$ th contact point. In utilizing these equations, the entire line of contact should be examined on a point-by-point basis to define the most critical contact point. Depending on the pitch of the tooth, 10 to 25 divisions should be adequate. For hand calculations, this could be quite burdensome. A quick look at the highest and lowest points of single-tooth contact (based on a transverse-plane slice of the helical set) will provide a reasonable approximation.

The range of materials and oils shown in Table 10.8 is limited. Generally, scoring is a problem only in high-speed, high-load applications.

The most likely applications to be affected are aerospace types. This being the case, the material choice is limited to those shown, and usually either MIL-L-23699 or MIL-L-7808 oil is used. Some of the new XAS-2354 oils will provide much improved scoring resistance, but hard data are not presently available.

## REFERENCES

---

- 10.1 ANSI/AGMA 2001-C95, "Fundamental Rating Factors and Calculation Methods for Involute Spur and Helical Gear Teeth."
- 10.2 "Design Guide for Vehicle Spur and Helical Gears," AGMA publ. 6002-B93.
- 10.3 *Gear Handbook*, vol. 1, *Gear Classification, Materials, and Measuring Methods for Unassembled Gears*, AGMA publ. 2000-A88.
- 10.4 Raymond J. Drago, "Results of an Experimental Program Utilized to Verify a New Gear Tooth Strength Analysis," AGMA publ. 229.27, October 1983.
- 10.5 Raymond J. Drago, "An Improvement in the Conventional Analysis of Gear Tooth Bending Fatigue Strength," AGMA publ. 229.24, October 1982.
- 10.6 R. Errichello, "An Efficient Algorithm for Obtaining the Gear Strength Geometry Factor on a Programmable Calculator," AGMA publ. 139.03, October 1981.
- 10.7 D. Dowson, "Elastohydrodynamic Lubrication: Interdisciplinary Approach to the Lubrication of Concentrated Contacts," NASA SP-237, 1970.
- 10.8 E. J. Wellauer and G. Holloway, "Application of EHD Oil Film Theory to Industrial Gear Drives," ASME paper no. 75PTG-1, 1975.
- 10.9 "Information Sheet—Gear Scoring Design Guide for Aerospace Spur and Helical Involute Gear Teeth," AGMA publ. 217.